

Cosmic UHE Tau Neutrinos and Implications

Ina Sarcevic*
University of Arizona

- Astrophysical Sources of UHE Neutrinos
- Cosmic Tau Neutrinos from $\nu_\mu \rightarrow \nu_\tau$ Oscillations over Astrophysical Distance
- ν_μ and ν_τ Interactions and Propagation through Earth
- High Energy Muon and Tau Propagation through Earth
- Detection of Cosmic UHE Neutrinos with ICECUBE and ANITA
- UHE Neutrinos as Probes of Physics Beyond the Standard Model

*Iyer, Reno and I. S., Phys. Rev. D61, 053003 (2000); Phys. Rev. D62, 123001 (2000); Phys. Rev. D64, 113001 (2001); Iyer Dutta, Reno, Seckel and I. S., Phys. Rev. D63, 094020 (2001); Iyer Dutta, Reno and I. S., Phys. Rev. D66, 077302 (2002); Phys. Rev. D66, 033002 (2002); Jones, Mocioiu, Reno and I. S., Phys. Rev. D69, 033004 (2004); Reno, I. S. and Su, hep-ph/0503030.

High Energy Neutrino Interactions

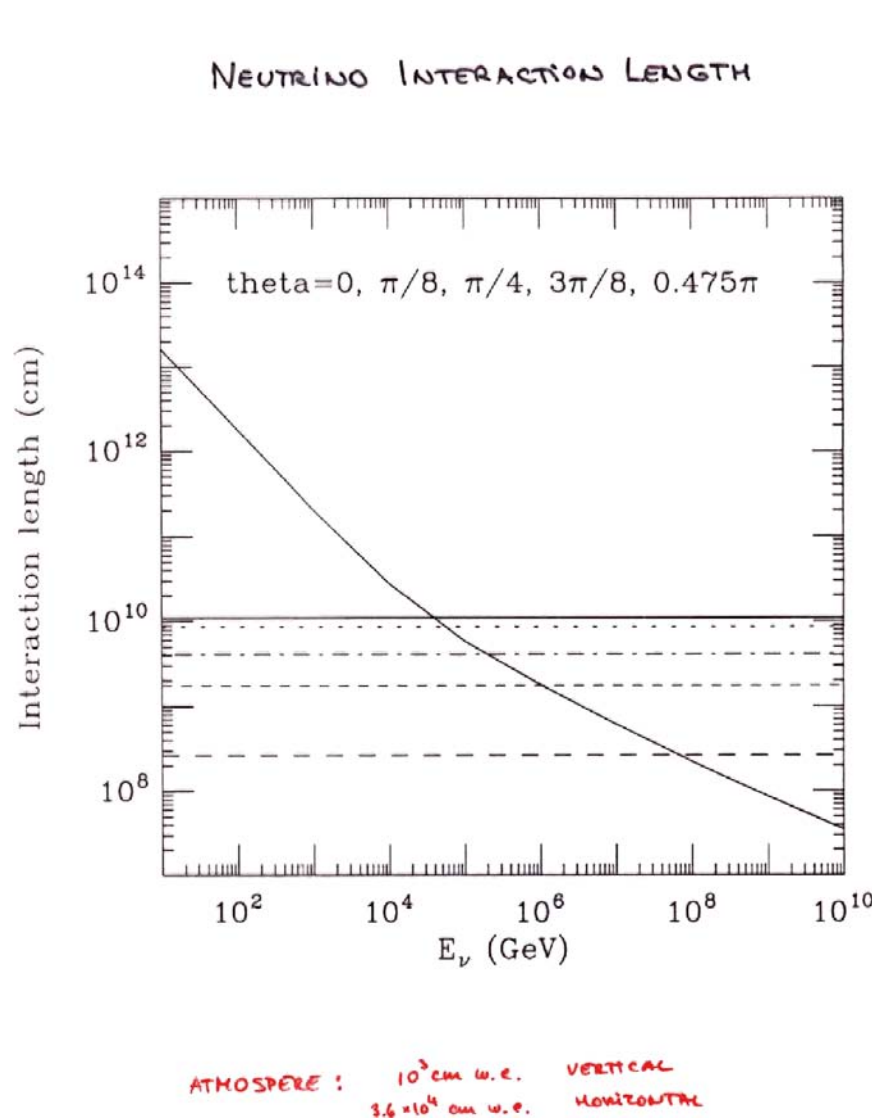
- Neutrinos are highly stable, neutral particles \Rightarrow Thus cosmic neutrinos point back to astrophysical point sources and bring information from processes otherwise obscured by a few hundred gm of a material.
- Interaction length of a neutrino is

$$\mathcal{L}_{\text{int}} \equiv \frac{1}{\sigma \cdot N_A}$$

Interaction length of 1TeV neutrino is 250 kt/cm² or column of water of 2.5 million km deep.

- Neutrino astronomy could provide a unique window into the deepest interiors of stars and galaxies (HE photons get absorbed by a few hundred gm of a material).

Neutrinos: a new window to the Universe



Sources of very high energy neutrinos

- * Cosmogenic ("GZK") neutrinos (interactions of cosmic rays with microwave background radiation)

- * Active Galactic Nuclei (AGN)

- * Gamma Ray Bursts (GRB's)

- * Z burst

- * ...

Sources of UHE Neutrinos

- **Cosmogenic Neutrinos**

Neutrinos produced by high energy cosmic rays interacting with the microwave background radiation (photoproduction followed by pion decay).

- **Neutrinos from AGNs**

AGNs are believed to be prodigious particle accelerators and the most powerful radiation sources known in the Universe, with luminosities ranging from $10^{42} - 10^{48}$ erg/s. If the observed TeV gamma rays (from **Mkn 421** and **Mkn 501**) originate in the decay of π^0 , then AGNs may also be the most powerful sources of UHE neutrinos.

- **Neutrinos from GRBs**

The cosmological GRB fireball energy is expected to be converted by photo-meson production to a burst of high energy neutrinos.

- Basic processes of neutrino production in extragalactic sources:

$$p + \gamma \rightarrow n + \pi^+$$

$$\hookrightarrow n + \gamma \rightarrow p + \pi^-$$

$$\hookrightarrow \pi^\pm \rightarrow \mu^\pm + \nu_\mu$$

$$\hookrightarrow \mu^\pm \rightarrow e^\pm + \nu_\mu + \nu_e$$

$$p + \gamma \rightarrow p + \pi^0$$

$$\hookrightarrow \pi^0 \rightarrow \gamma\gamma$$

- For astronomical distances ($L \sim 1000 Mpc$) and with $\Delta m^2 \sim 10^{-3} eV^2$

$$< \sin^2\left(\frac{1.27\Delta m^2 L(Km)}{E(GeV)}\right) > = \frac{1}{2}$$

(For PeV neutrinos potentially sensitive to $\Delta m^2 \sim 10^{-17} eV^2$!)

- The probability for $\nu_\mu \rightarrow \nu_\tau$ oscillations is given by

$$P(\nu_\mu \rightarrow \nu_\tau; L) = \sin^2 2\theta \sin^2\left(\frac{1.27\Delta m^2 L(Km)}{E(GeV)}\right)$$

- For large mixing angles, $P(\nu_\mu \rightarrow \nu_\tau; L) = 1/2$, i.e. $F_{\nu_\mu} = F_{\nu_\tau}$

- The observed photon energy spectrum is a power-law:

$$\frac{dN_\gamma}{dE_\gamma} \approx E_\gamma^{-2}$$

for $100\text{MeV} \leq E_\gamma \leq 2\text{TeV}$

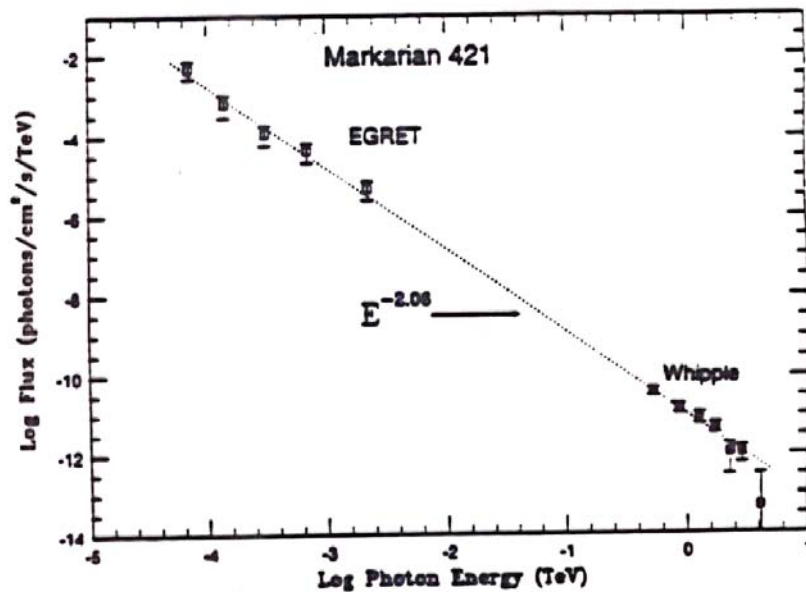
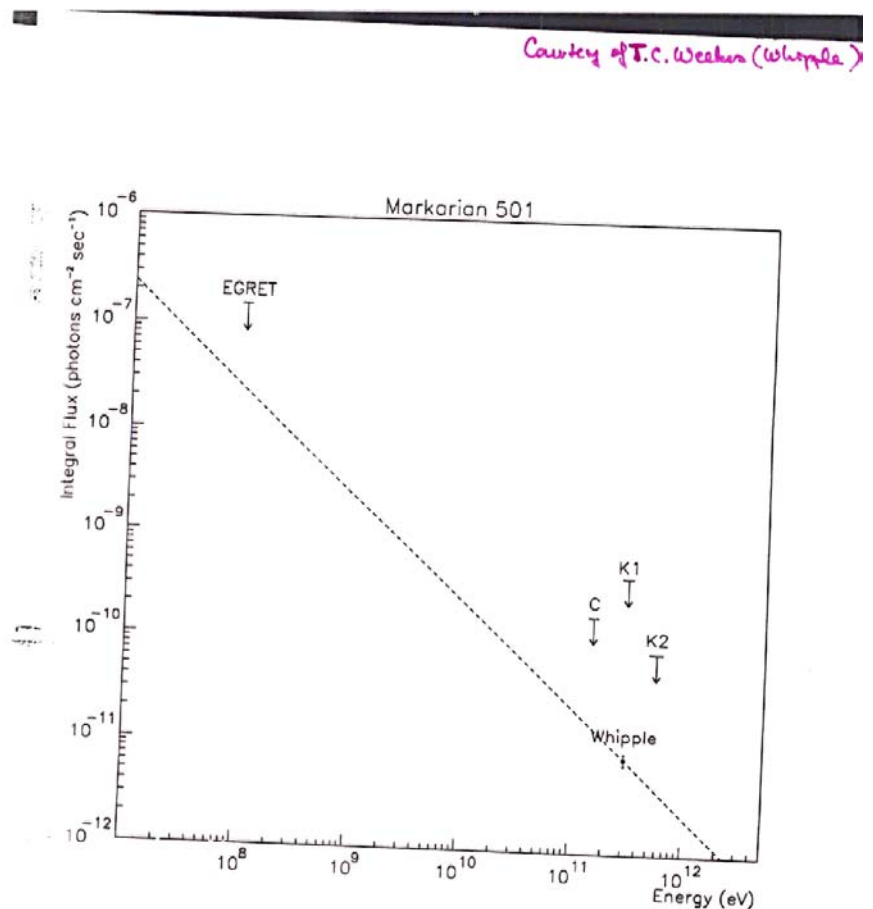


Figure 2. Differential energy spectrum from both the EGRET (Lin et al. 1992) and Whipple observations of Markarian 421. The EGRET observations were taken 27 June - 11 July, 1991; the Whipple observations 24 March - 2 June 1992. A single power-law, with energy exponent 2.06 ± 0.04 , is an acceptable description of the combined dataset. Possible systematic errors in the exponent are not included. They are difficult to estimate because of the differing technique by which the fluxes have been measured and because of the non-contemporaneous nature of the observations.



Active Galactic Nuclei (AGN)

- Radio loud quasars in elliptical host galaxies, often have jets.
- Radio quiet quasars in the core of spiral galaxies.
- Several AGN detected γ -rays in TeV energy range:
 - 5 in Northern Hemisphere:
 - ★ Mkn 421 (z=0.0300); $\alpha = 2.1$
 - ★ Mkn 501 (z=0.033)
 - ★ 1ES 2344+514 (z=0.044)
 - ★ 1ES 1959+650 (z=0.048)
 - ★ 1ES 1426+428 (z=0.129)
 - 1 in Southern Hemisphere:
 - ★ PKS 2155-304 (z=0.116); $\alpha = 3.3$
 - ★ PKS 2005-4899 (z=0.071); $\alpha = 4.0$



- Structure of the hadronic cascade:

$$pp \rightarrow \pi + X$$

$$p\gamma \rightarrow \pi + X$$

$$np \rightarrow \pi + X$$

$$\pi^0 \rightarrow \gamma + \gamma$$

$$\pi^\pm \rightarrow \nu_\mu + \mu$$

$$\mu \rightarrow \nu_\mu + \nu_e + e$$

- Neutrino spectrum from a single source mirrors the spectrum of the protons and the diffuse AGN neutrino flux obtained by NMB is given by:

$$\frac{dN_{\nu_\mu + \bar{\nu}_\mu}}{dE_\nu} = 1.1 \times 10^{-12} (E_\nu (\text{TeV}))^{-2} \text{cm}^{-2} \text{s}^{-1} \text{sr}^{-1} \text{GeV}^{-1}$$

- $\nu_e + \bar{\nu}_e$ spectrum is assumed to be 1/2 of $\nu_\mu + \bar{\nu}_\mu$
- Neutrino luminosity of a source is normalized to the observed diffuse x-rays and γ -rays.
- Uncertainty: What fraction of the observed x-rays originate in hadronic cascade?

- It seems plausible that protons generated within an AGN interact with matter or radiation in the AGN disk, or with UV photons in the associated jets, to produce pions whose decay products include PHOTONS and NEUTRINOS

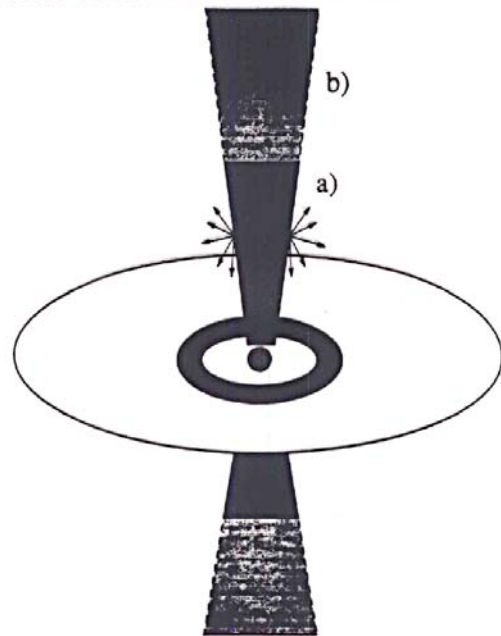


FIG. 1. Schematic diagram of the central engine of an AGN (not to scale). A supermassive black hole at the center is surrounded by an accretion disk of gas falling into the black hole. Two jets of plasma are ejected perpendicular to the disk. Typically, shocks form in the jets. In such shocks (wavy line), protons are accelerated, which eventually leave the jet and drift back to the disk. In the inner region (dark ring, $\approx 10R_S$ to $\approx 200R_S$), protons reaching the disk initiate cascades through $p\gamma$ interactions. Only protons accelerated in the outer region (b) of the jet can reach energies above the threshold for $p\gamma$ reactions with UV photons.

Say a Telescope (1992)

ACTIVE GALACTIC NUCLEI: SORTING OUT THE MESS

BY ANN FINKBEINER

MOST GALAXIES are bright in their centers, but decorously so. "Active" galaxies, on the other hand, have centers that are immodestly bright. Dazzling light from a tiny nucleus all but swamps the rest of the galaxy. In fact active galactic nuclei, or AGNs as they are called, are the brightest things in the universe.

AGNs come in a bewildering variety of forms. In recent years, however, our picture of them has been growing simpler and clearer, just as their role in the cosmos is assuming new importance.

Only about one percent of galaxies have active nuclei. But over the history of the universe, these objects have produced nearly as much energy as all galaxies combined. And, strangely, most of that bright light cannot be coming from stars. Stars give off most of their energy in a rather narrow range of wavelengths, from mid-ultraviolet to mid-infrared, but AGNs shine across the entire spectrum, from radio to gamma-ray wavelengths. Whatever is lighting them up is not what lights up most of the rest of the universe.

Other properties of AGNs are equally extreme. They change brightness substantially on all time-scales from minutes to at least decades. Some send out spectacular squirts of gas millions of light-years long. A few are relatively close by, but most (including the extremely luminous ones) inhabit the distant and early universe; they were far more common then than they are now. In fact AGNs are the earliest congregations of matter known — the visible

Only about one percent of galaxies have active nuclei. But over the history of the universe, these objects have produced nearly as much energy as all galaxies combined.

signs of the first systems to coalesce after the Big Bang.

Since the early 1940s astronomers have been collecting these extravagant characters and classifying them under various names: Seyfert 1 and Seyfert 2 galaxies, broad-line and narrow-line radio galaxies, radio-loud and radio-quiet quasars, optically violent variable quasars, and BL Lacertae objects. Until recently, however, astronomers hadn't much sense of whether the different types of AGNs were related, what they were, or how they worked. "We had been doing botany," says C. Megan Urry, an astronomer at the Space Telescope Science Institute who specializes in active galaxies. "and now we're undoing that mess."

Undoing the mess means astronomers now more or less agree that all AGNs are different aspects of the same phenomenon. The theory is simple: AGNs look different only because we see the same type of object tilted at different an-

gles on the sky. Astronomers also agree that the power source underlying them all is probably a supermassive black hole violently sucking in quantities of gas. The relatively tiny black hole and its hot surroundings lie within a large, thick torus, a doughnut, of dust and cooler gas. This is turn is surrounded on all sides by larger cooler gas clouds spaced widely apart. The whole affair forms the nucleus of a galaxy.

There's no agreement yet on exactly how the AGN phenomenon works. But if astronomers are right about what AGNs are and once they figure out how AGNs function, these exaggerated objects might provide crucial evidence about the beginning and innermost workings of all galaxies.

THE FIRST SIGNS

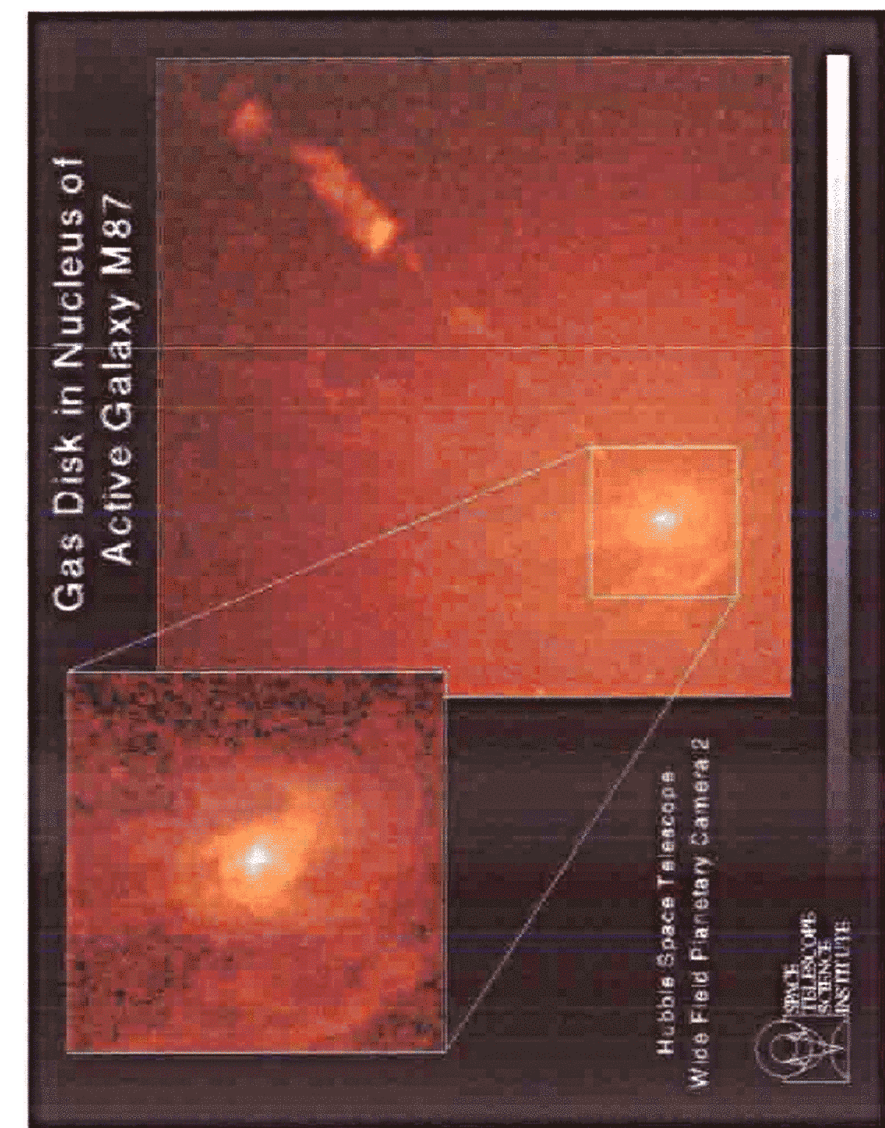
AGN collecting began 50 years ago when Rudolph Minkowski and Milton Humason at Mount Wilson Observatory handed over the spectra of several spiral galaxies with oddly bright centers to a postdoctoral student, Carl K. Seyfert. Spectra are little rainbows of an object's light spread out to display all its colors, or wavelengths. An astronomical object's spectrum is usually marked by many thin bright or dark lines that reveal volumes about conditions in and around the light source. Bright lines come from tenuous hot gas, dark ones from cooler gas through which the light passes. Usually the spectral lines are very thin, but sometimes they are broadened because the gas is especially hot or moving rapidly.

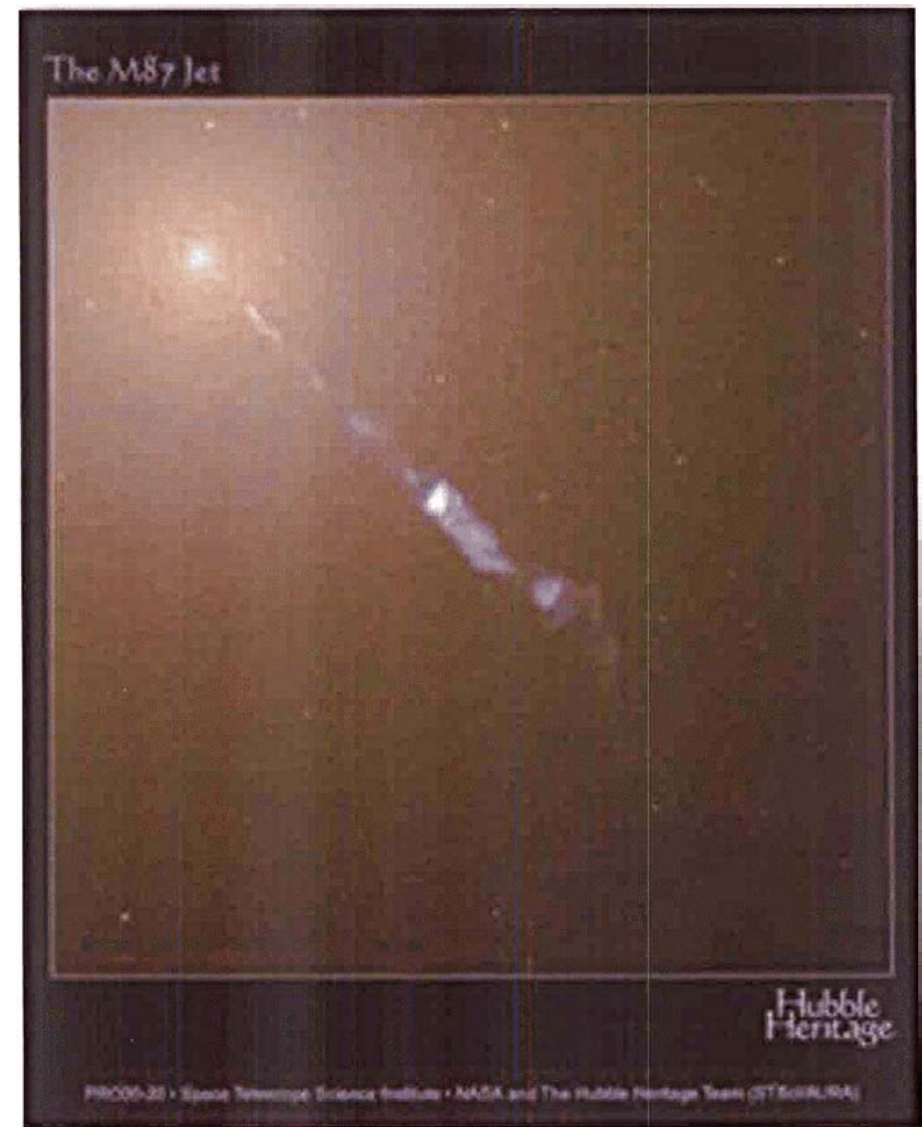
Normally the spectra of spiral galaxies

AGN SS flux → upper bound for AGN core emission
(difusse X-ray background)

flux above 1 PeV may be reduced due to cooling of pions
and muons in the strong magnetic fields of AGN

M_95A flux → upper bound for AGN jet emission
model
(extragalactic γ -ray background)





Gamma Ray Bursts (GRBs)

- Fireball Model: GRB are produced by the dissipation of the kinetic energy of the relativistic expanding fireball with a large fraction ($> 10\%$) of fireball energy being converted by photo-pion production to HE neutrinos. HE protons accelerated in ultrarelativistic shocks interact with synchrotron photons inside the fireball.

$$F_{\nu+\bar{\nu}}^s(E) = 4.0 \times 10^{-\alpha} E^{-n},$$

where $\alpha = 13$ and $n = 1$ for $E < 10^5$ GeV and $\alpha = 8$, $n = 2$ for $10^5 < E < 10^7$ GeV and $n = 3$ for $E > 10^7$ GeV.

Waxman-Bahcall, *Phys. Rev. D* 59, 023002 (1999)

- Recently another mechanism was proposed for producing TeV neutrinos, from choked relativistic fireball jets that are unable to punch through the stellar envelope. These neutrinos appear as precursor signal, tens of seconds prior to the observations of γ rays produced outside the star by a collapsing massive star induced GRB. The predicted neutrino flux is given by:

$$F_{\nu+\bar{\nu}}^s(E) = 10^{-7} E^{-2}$$

Meszaros and Waxman, *PRL* 87 (2001)

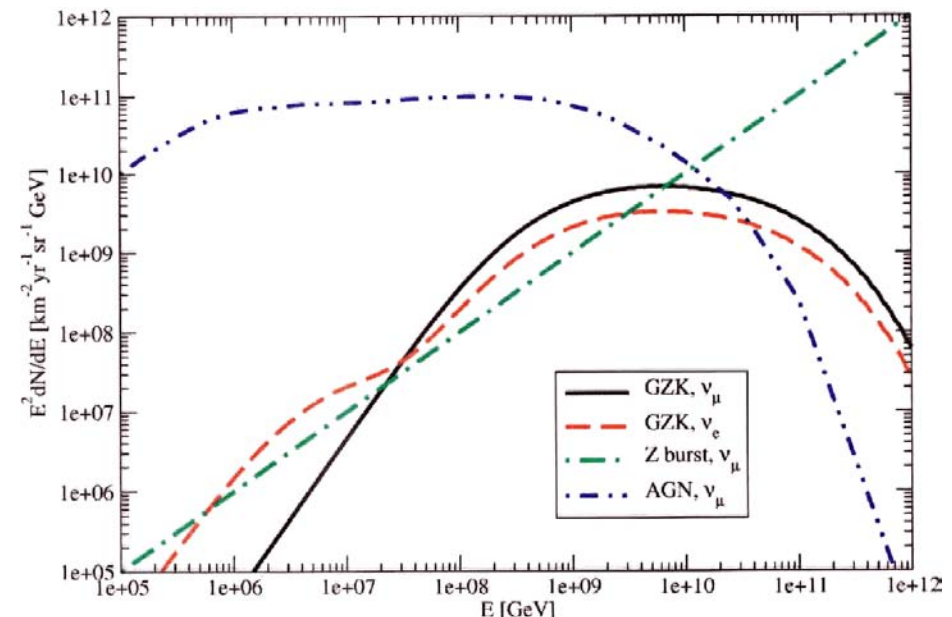
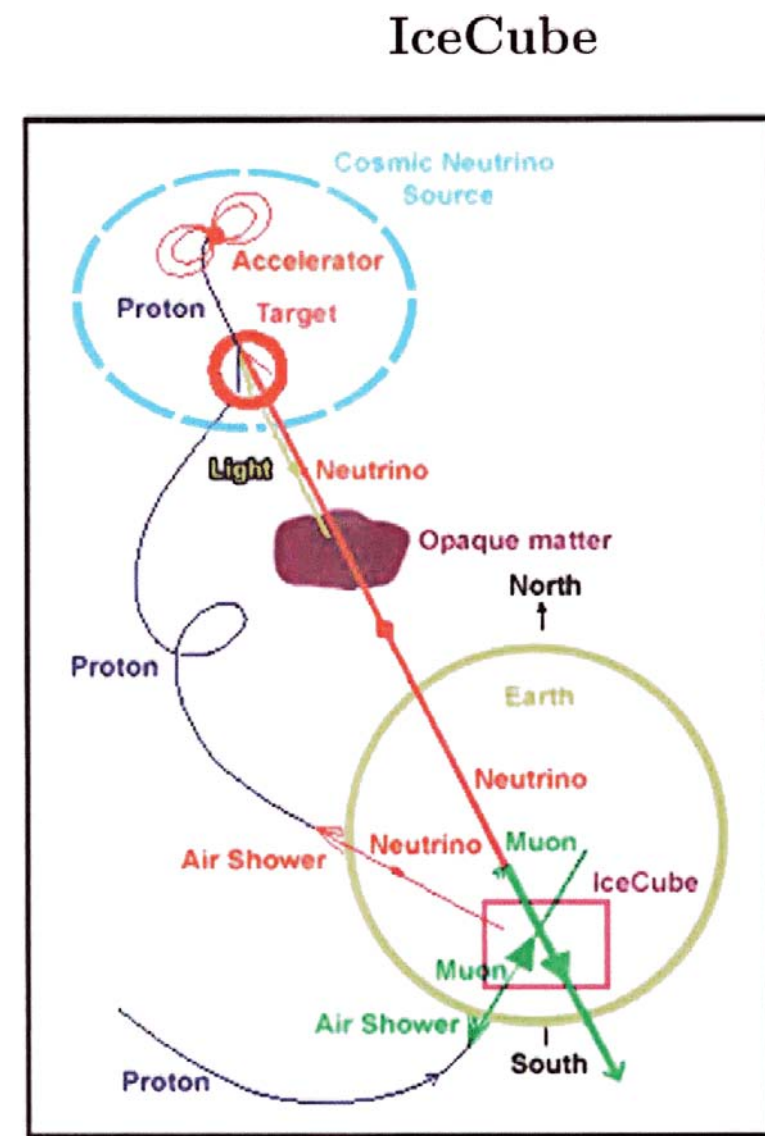
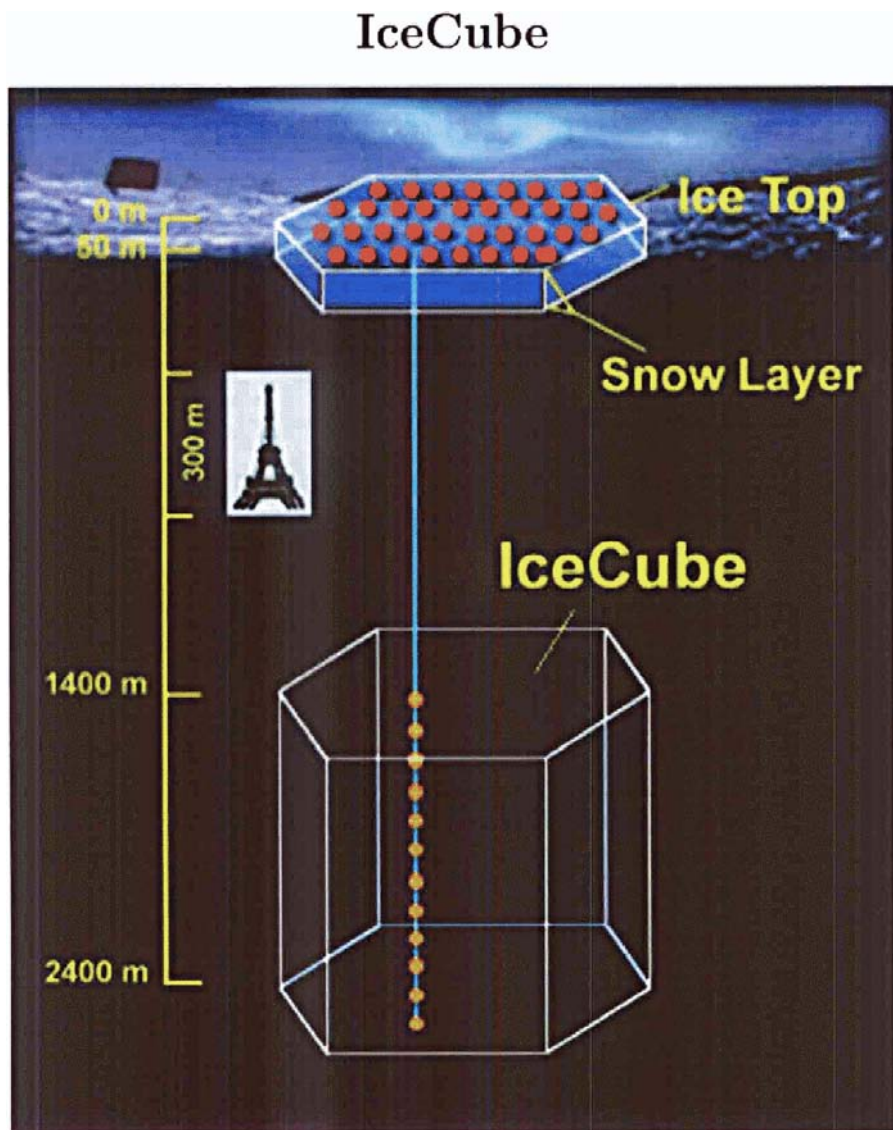


Figure 1: Initial Neutrino Fluxes.

Experiments

- AMANDA / ICECUBE / ICECUBE-PLUS / HYPERCUBE
- ANTARES, NESTOR
- RICE
- ANITA
- PIERRE AUGER
- EUSO, OWL
- SalSA, LOFAR ...





ANITA: Antarctic Impulsive Transient Antenna



Science Objectives: Detection of ultra-high energy cosmic neutrinos

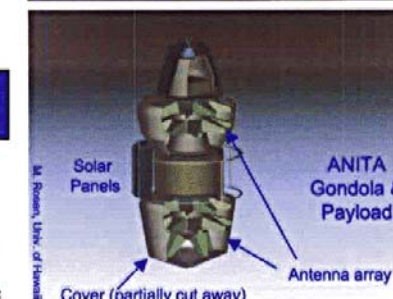
ANITA addresses NASA Structure and Evolution of the Universe (SEU) themes:

- Examines the *ultimate limits of energy in the universe* by measurements of completely new kinds of energetic particles: **neutrinos**, which are the only known ultra-high-energy particles that are able to reach earth unabsorbed from cosmological distances
- Probes the *nature and origin of the highest energy cosmic rays*, via the most sensitive observation to date of their characteristic neutrino by-products.



A cutaway view of Antarctic ice sheet: ANITA observations penetrate deep into the ice itself. Balloon flight path is shown.

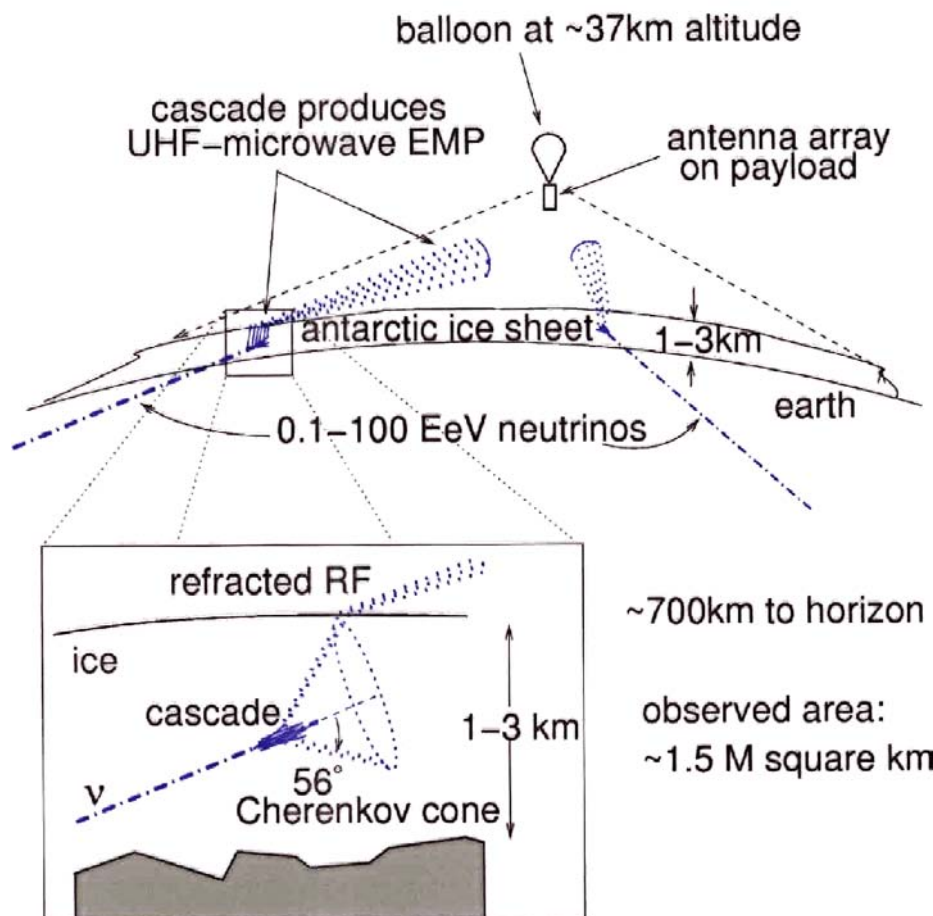
Science Payload: 36 Dual-Polarized Antennas covering 0.3-1.5 GHz



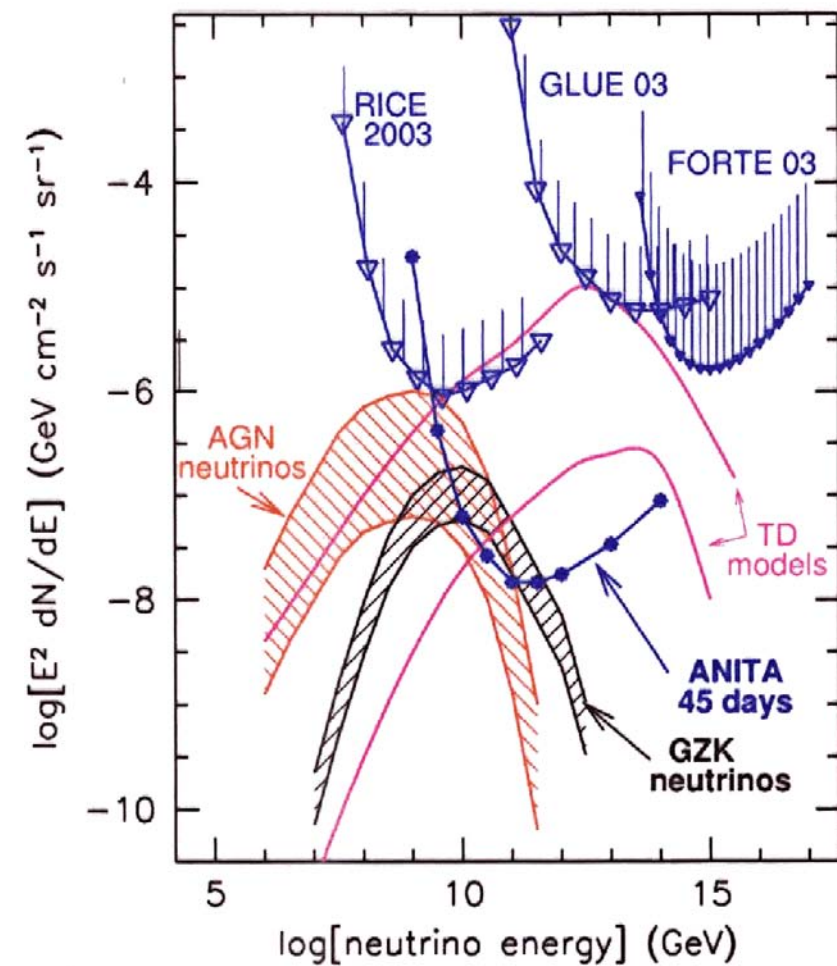
Mission Overview: A long-duration balloon mission over Antarctica

- First flight in 2004-2005, two additional flights in 05-06, 06-07
- Each Flight: 9-12 days; Baseline Mission plan: 30 days total flight time
- Radio-frequency monitoring of Antarctic ice sheet from ~40 km altitude
- Flights are circumpolar due to continuous wind circulation around south pole
- Neutrino cascades within ice sheet produce strong Electro-magnetic pulse (EMP) which propagates through ice
- Antarctic ice is transparent to radio waves up to ~1-1.5 GHz
- Ice sheet becomes a neutrino "converter:" neutrinos enter and radio waves come out.
- Effective telescope area: ~1M km² !
- Array of low-gain log-periodic antennas views ice sheet out to ~680 km
- Utilize Askaryan effect in neutrino cascades: radio pulse mechanism tested at accelerators
- ~10° azimuth resolution via antenna beam gradiometry within antenna clusters
- ~3° elevation resolution by interferometry between top & bottom antenna clusters
- Pulse polarimetry to get additional information on neutrino direction

ANITA



ANITA



The diagram shows the Earth from space, with several small white dots representing the OWL satellite in orbit. A large blue cone, representing the field of view or sensitivity of the detector, is centered on the Earth. The text on the slide includes:

**Orbiting Wide-angle Light collectors
OWL**

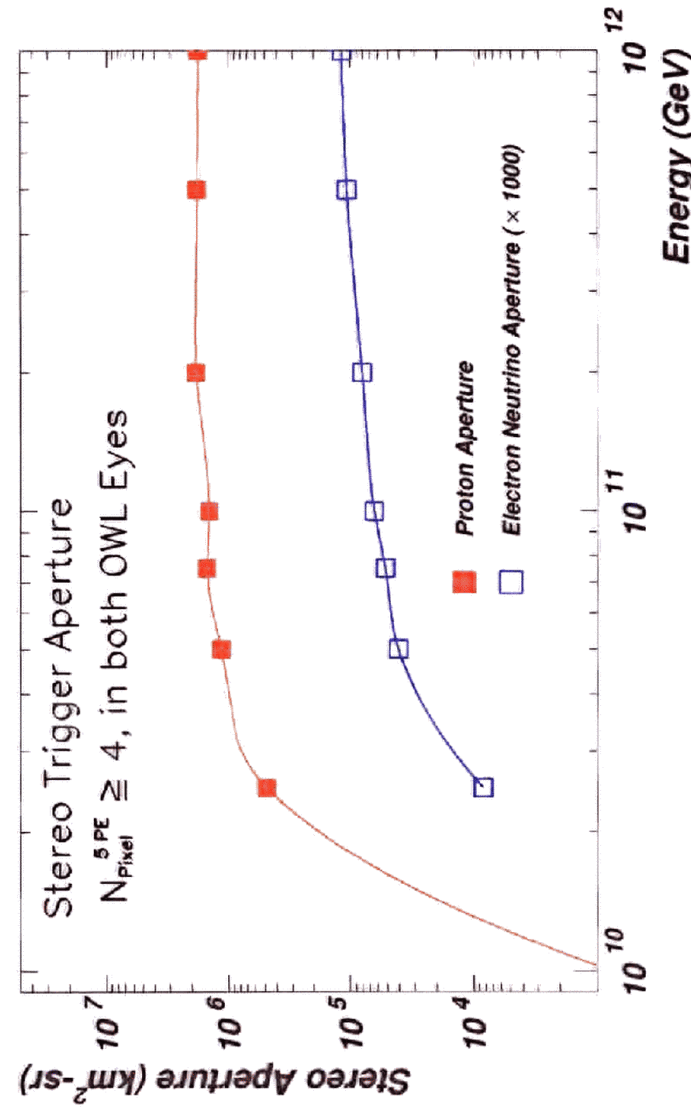
An Earth Orbiting System to Study Air Showers Initiated by
 $>10^{19}$ eV Particles

- Earth as calorimeter
- Nitrogen fluorescence
- Monitor 3 million Km²
- 3000 events/year

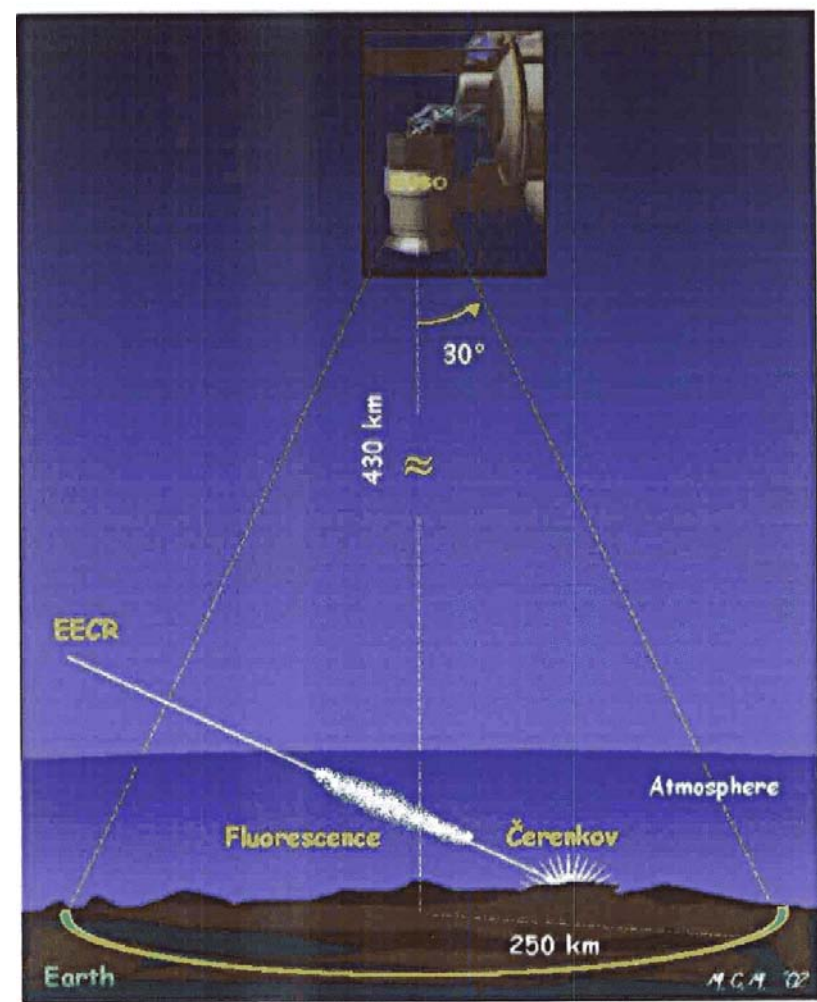


OWL

OWL



EUSO



AUGER



SALSA: rock salt formations as large scale neutrino detectors (salt has a higher density than ice, so it is possible to achieve an effective detection volume of several hundred km³ water equivalent in salt) Threshold for detecting the radio signal from showers in salt is of the order of $\sim 10^7$ GeV.

LOFAR: a digital telescope array designed to detect radio Cherenkov emission in air showers with sensitivity in an energy range of $\sim 10^5 - 10^{11}$ GeV. With its low energy threshold, LOFAR has an excellent opportunity to observe the shower enhancement at lower energies due to ν_τ regeneration and tau pileup, which is not easily accessible in ANITA.

- As ν_μ 's propagate through the Earth, their flux get attenuated while ν_τ 's get regenerated via τ decay

$$\nu_\mu + N \rightarrow \mu + X$$

and muons get absorbed, while

$$\nu_\tau + N \rightarrow \tau + X$$

followed by the τ decaying back into ν_τ

$$\tau \rightarrow \nu_\tau + X$$

(muon lifetime: $\tau_\mu = 2.2 \times 10^{-6} s$)

(tau lifetime: $\tau_\tau = 2.9 \times 10^{-13} s$)

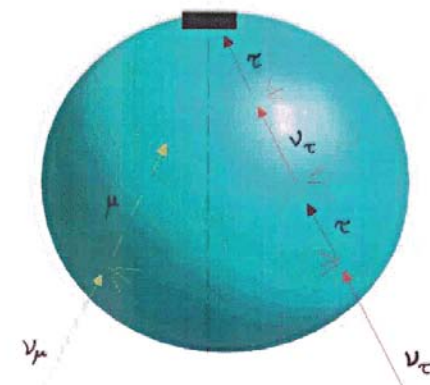
tau decay length:

$$\rho_\tau^{dec}(E, X) = \gamma \tau_\tau \rho(X)$$

- Tau charged-current interaction length and the photonuclear interaction length become comparable to the tau decay length at $E > 10^8$ GeV

- Qualitative behavior of ν_τ is different than ν_μ in propagation through Earth

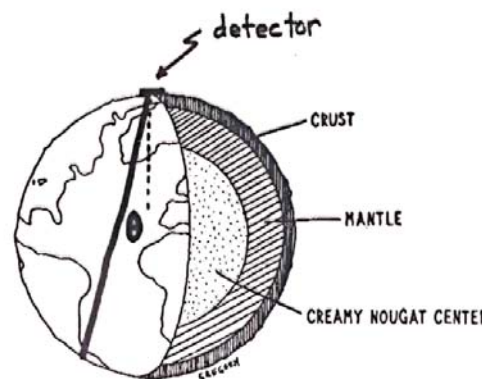
(Halzen and Saltzberg, PRL 81 (1998))



- Main difference due to lifetimes:

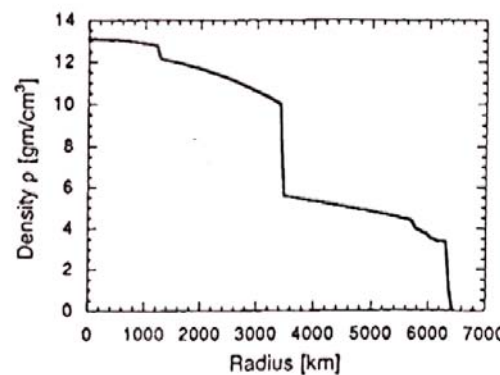
$$\tau_\mu = 2.2 \times 10^{-6} s$$

$$\tau_\tau = 2.9 \times 10^{-13} s$$



χ = column depth [g/cm²]

θ = nadir angle



Preliminary Earth Model

- For energies above 10^6 GeV, of relevance to OWL/EUSO, RICE and ANITA, we need to include the energy loss of the τ propagating through the Earth.

- Energy loss processes for muons and taus:

- ★ Bremsstrahlung
- ★ Ionization
- ★ Pair Production
- ★ Photonuclear Processes

S.I. Dutta, M.H. Reno, I. Sarcevic and D. Seckel, PRD63, 094020 (2001).

S.I. Dutta, I. Mocioiu, J. Jones, M.H. Reno and I. Sarcevic, (2003).

- For energies above 10^6 GeV, new physics might become relevant, such as exchange of bulk gravitons (i.e. Kaluza-Klein modes) in the neutral-current interactions.

(Fig)

- Possibility of testing theory of large extra dimensions with ultrahigh energy neutrinos?

S. Nussinov and R. Shrock, PRD59, 105002 (1999); PRD64, 47702 (2001).
 P. Jain, D.W. McKay, S. Panda and J. Ralston, PLB484, 267 (2000).
 C. Tyler, A. Olinto and G. Sigl, PRD63, 055001 (2001).
 H. Davoudiasl, J.L. Hewett and T.G. Rizzo, PLB549, 267 (2002).

FIGURES

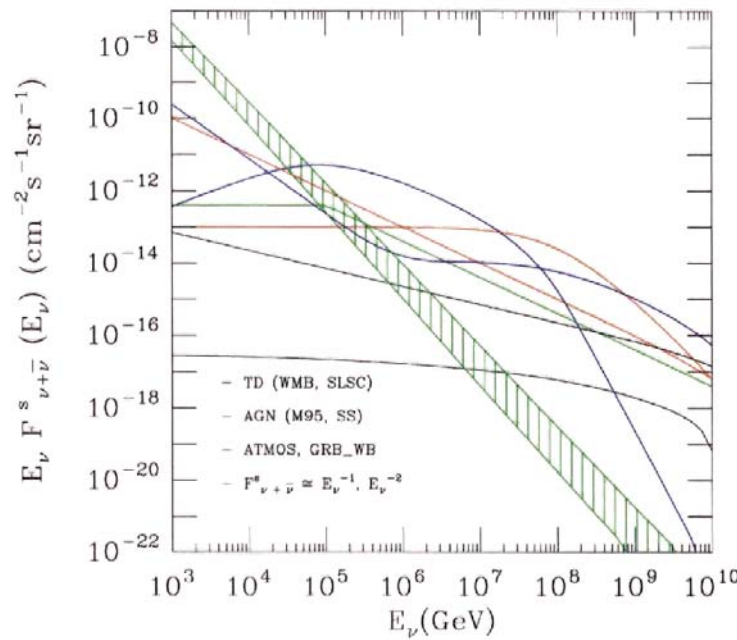
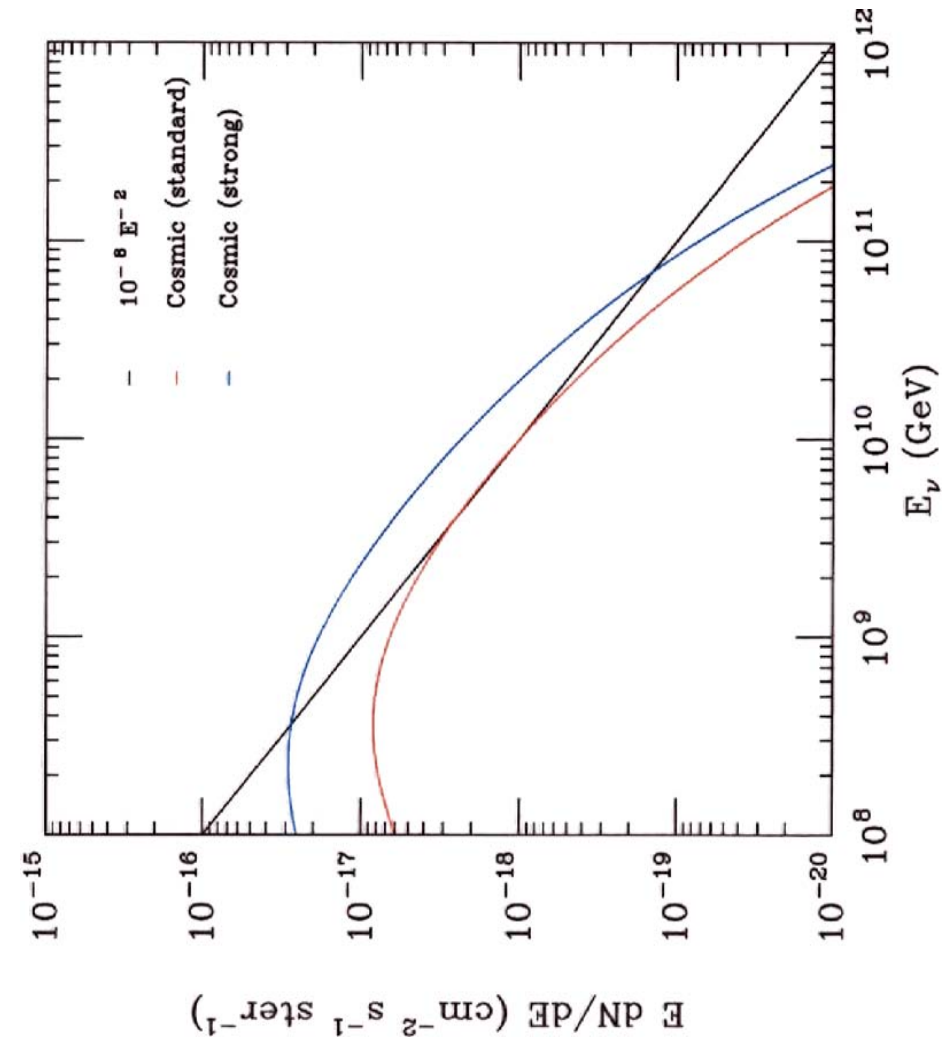


FIG. 1. Muon neutrino plus antineutrino fluxes for AGN models (blue lines, upper curve at low energy corresponds to AGN_M95, while the lower curve is for AGN_SS model), GRB (green line), topological defects models (black lines, upper curve corresponds to the TD_WMB, while the lower curve is for TD_SLSC), E^{-1} flux (lower red line at low energy) and E^{-2} (upper red line at low energy) and angle-dependent atmospheric (ATM) flux (green shaded area).

1



Neutrinos from Topological Defects

- Topological defects: monopoles, cosmic strings, domain walls, and superconducting cosmic strings, might have been formed in symmetry-breaking phase transitions in the early Universe.
 - * In the so-called "top-down" (TD) models, γ -rays, electrons (positrons), and neutrinos are produced directly at UHEs by the cascades initiated by the decay of a supermassive elementary "X" particle associated with some Grand Unified Theory (GUT), rather than being accelerated (i.e. TD might constitute a "nonacceleration" source of UHE neutrinos). The X particle are usually thought to be released from topological monopoles left over from GUT phase transition and it decays into quarks, gluons, leptons.
- Predicted spectra are much harder and extend much further beyond 100EeV than shock acceleration spectra.
- TD might be responsible for the highest energy events observed ($E \sim 10^{21}$ eV) → Fly's Eye and AGASA Experiments (Fig.)

Topological Defects Models:

Sigl-Lee-Schramm-Coppi (SLSC)

Wichoski-MacGibbon-Brandenberger (WMB)

- Energy loss of the string network converted into gravitational radiation or particle production
- Upper limits from cosmic ray data (Frejus, Fly's Eye)
- Upper limit for strong source evolution

$$2 \times 10^{-8} E^{-2}$$

Neutrino flavors

- source: π decays $\Rightarrow \nu_e : \nu_\mu : \nu_\tau = 1 : 2 : 0$
- propagation towards Earth: neutrino oscillations
 - * ν_μ and ν_τ maximally mixed $\Rightarrow \nu_e : \nu_\mu : \nu_\tau = 1 : 1 : 1$
- If $F_{\nu_e}^0 : F_{\nu_\mu}^0 : F_{\nu_\tau}^0 \neq 1 : 2 : 0$ then three flavor mixing is relevant

$$F_{\nu_e} = F_{\nu_e}^0 - \frac{1}{4} \sin^2 2\theta_{12} (2F_{\nu_e}^0 - F_{\nu_\mu}^0 - F_{\nu_\tau}^0)$$

$$F_{\nu_\mu} = F_{\nu_\tau} = \frac{1}{2} (F_{\nu_\mu}^0 + F_{\nu_\tau}^0) + \frac{1}{8} \sin^2 2\theta_{12} (2F_{\nu_e}^0 - F_{\nu_\mu}^0 - F_{\nu_\tau}^0)$$

J. Jones, I. Mocioiu, M.H. Reno and I.S.,
Phys. Rev. D69, 033004 (2004).

Propagation through the Earth/ice

S. Iyer, M.H. Reno and I. S., PRD61 (2000);
S. Iyer Dutta, M.H. Reno and I. S., PRD62 (2000)
S. Iyer Dutta, M.H. Reno and I.S., PRD64 (2001); PRD66 (2002)

- ν attenuation due to charged (CC) and neutral current (NC) interactions
- NC return of ν
- regeneration of ν from τ decay

$$\begin{aligned} \frac{\partial F_{\nu_\tau}(E, X)}{\partial X} = & -N_A \sigma^t(E) F_{\nu_\tau}(E, X) + N_A \int_E^\infty dE_y F_{\nu_\tau}(E_y, X) \frac{d\sigma^{NC}}{dE}(E_y, E) \\ & + \int_E^\infty dE_y \frac{F_\tau(E, X)}{\lambda_\tau^{dec}} \frac{dn}{dE}(E_y, E) \end{aligned}$$

- τ decay
- CC production of τ

$$\frac{\partial F_\tau(E, X)}{\partial X} = N_A \int_E^\infty dE_y F_{\nu_\tau}(E_y, X) \frac{d\sigma^{CC}}{dE}(E_y, E) - \frac{F_\tau(E, X)}{\lambda_\tau^{dec}(E, X, \theta)}$$

- τ energy loss

$$-\frac{dE_\tau}{dX} = \alpha_\tau + \beta_\tau E_\tau$$

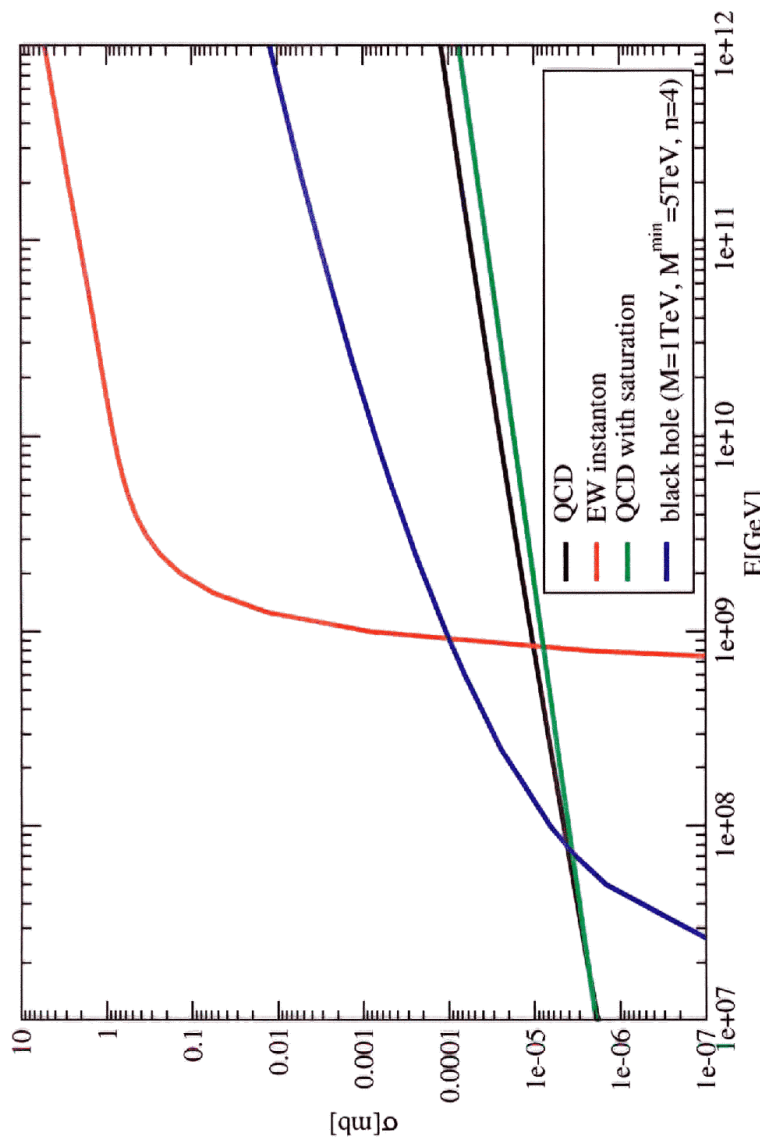
S. Iyer Dutta, M.H. Reno, D. Seckel and I. S., PRD63 (2001)

High Energy Neutrino Propagation and Small x Parton Distributions

- Ultrahigh energy neutrino cross section depends on parton distributions at very small x , values that are beyond currently accessible range in the colliders.
- In order to obtain charged-current and neutral-current neutrino cross sections at energies above 10^6 GeV , we need to extrapolate parton distribution into the low x region.
- Three approaches to the extrapolation:
 - * extrapolation of the standard DGLAP evolution
 - * unified BFKL/DGLAP evolution equations
 - * inclusion of saturation effects, via nonlinear terms in BFKL/DGLAP equations
- Standard gluon distribution obtained within the DGLAP framework from the global fit, such as MRS or CTEQ, extended to lower values of x using the power-law extrapolation.
- The BFKL framework resums the leading terms $\alpha_s \ln 1/x$, NLO corrections and has the advantage of treating both the BFKL

and DGLAP evolution schemes on equal footing. In this framework one is using the high energy factorization theorem together with the unintegrated parton distribution function.

- In the region of high energies, where the parton densities become high, the parton recombination effects can become important. These effects lead to the slower increase of the parton density with energy and in consequence to the damping of the cross section. This is called *a perturbative parton saturation*. These effects are included via nonlinear terms in BFKL/DGLAP evolution equation.
- The effect of small x extrapolations on neutrino flux as it propagates through rock and on electromagnetic showers in ice, with DGLAP parton distribution and with nonlinear BFKL/DGLAP is large for energies above 10^8 GeV .
- Consider angular distribution combined with energy distribution of neutrino induced electromagnetic and hadronic showers in ICECUBE, ANITA and Auger, in order to assess the sensitivity to small x parton distributions and study a possibility of determining the behavior of parton distributions at very small x . Knowing the behavior of parton distributions at very small values of x is crucial for physics at the LHC.



For neutrino energies in the range

$$10^{15} \text{ eV} \leq E_\nu \leq 10^{21} \text{ eV},$$

good numerical representations of the cross sections calculated using the CTEQ4–DIS parton distributions are given by simple power-law forms,

$$\sigma_{CC}(\nu N) = 4.305 \times 10^{-36} \text{ cm}^2 \left(\frac{E_\nu}{1 \text{ GeV}} \right)^{0.37299}$$

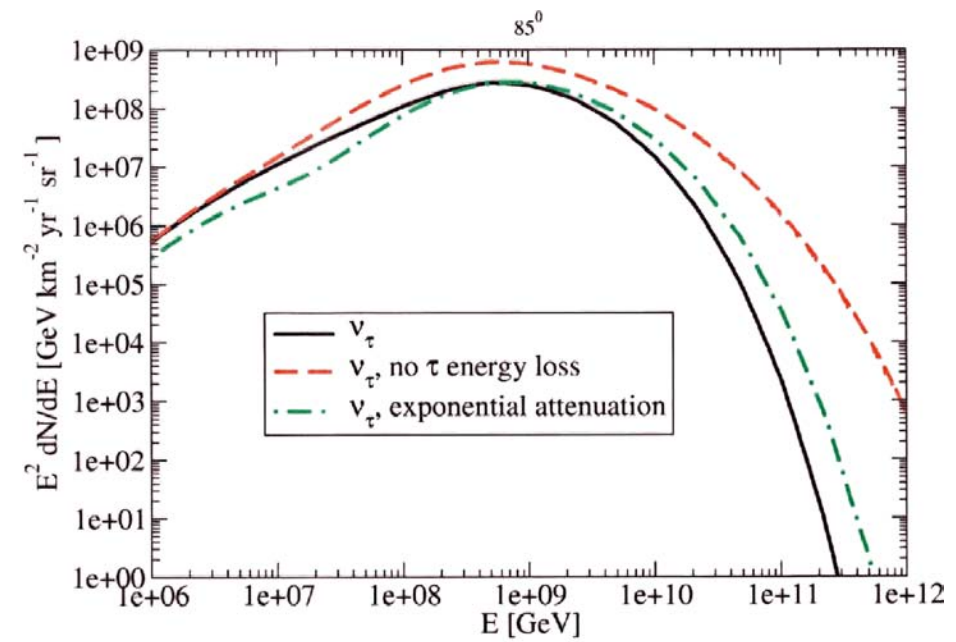
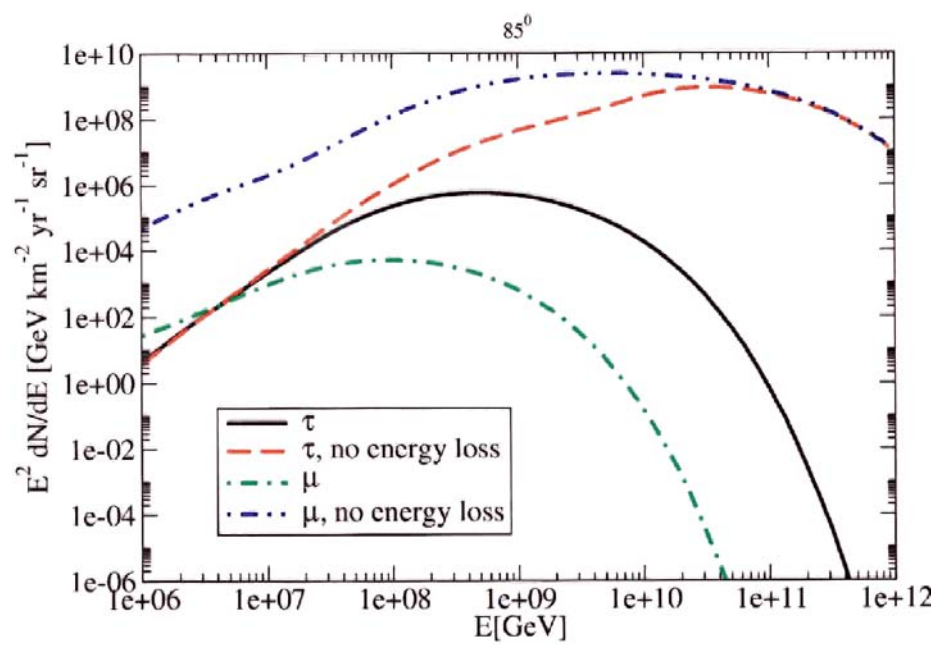
$$\sigma_{NC}(\nu N) = 1.712 \times 10^{-36} \text{ cm}^2 \left(\frac{E_\nu}{1 \text{ GeV}} \right)^{0.37753}$$

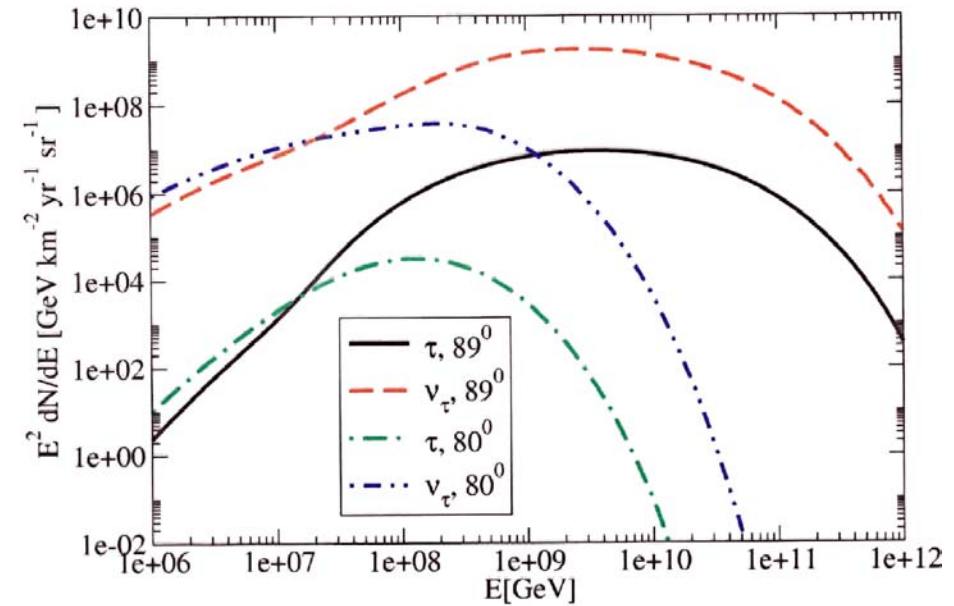
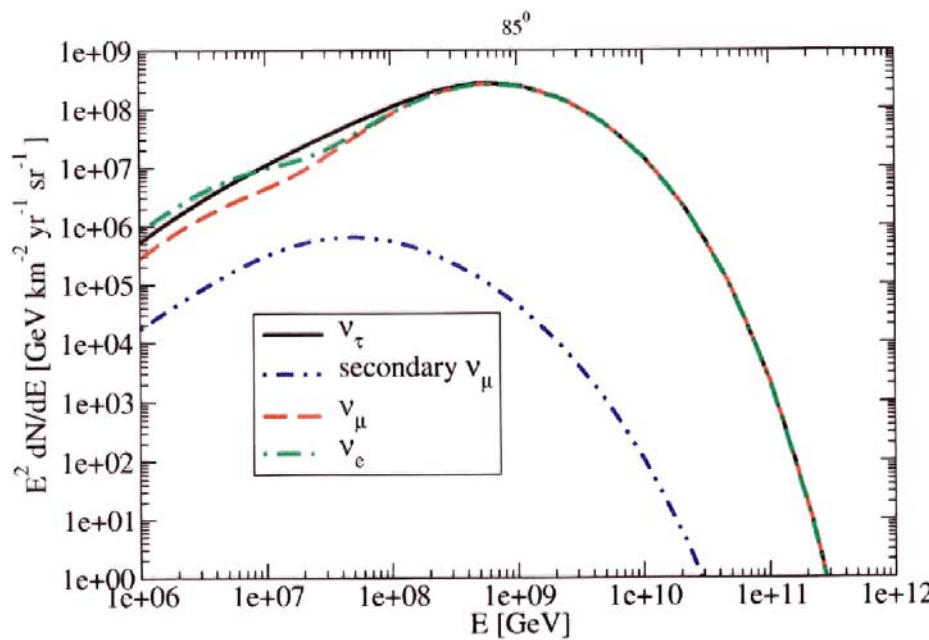
$$\sigma_{\text{tot}}(\nu N) = 6.0128 \times 10^{-36} \text{ cm}^2 \left(\frac{E_\nu}{1 \text{ GeV}} \right)^{0.37436}$$

$$\sigma_{CC}(\bar{\nu} N) = 4.319 \times 10^{-36} \text{ cm}^2 \left(\frac{E_\nu}{1 \text{ GeV}} \right)^{0.37231}$$

$$\sigma_{NC}(\bar{\nu} N) = 1.7276 \times 10^{-36} \text{ cm}^2 \left(\frac{E_\nu}{1 \text{ GeV}} \right)^{0.37658}$$

$$\sigma_{\text{tot}}(\bar{\nu} N) = 5.7819 \times 10^{-36} \text{ cm}^2 \left(\frac{E_\nu}{1 \text{ GeV}} \right)^{0.37598}$$





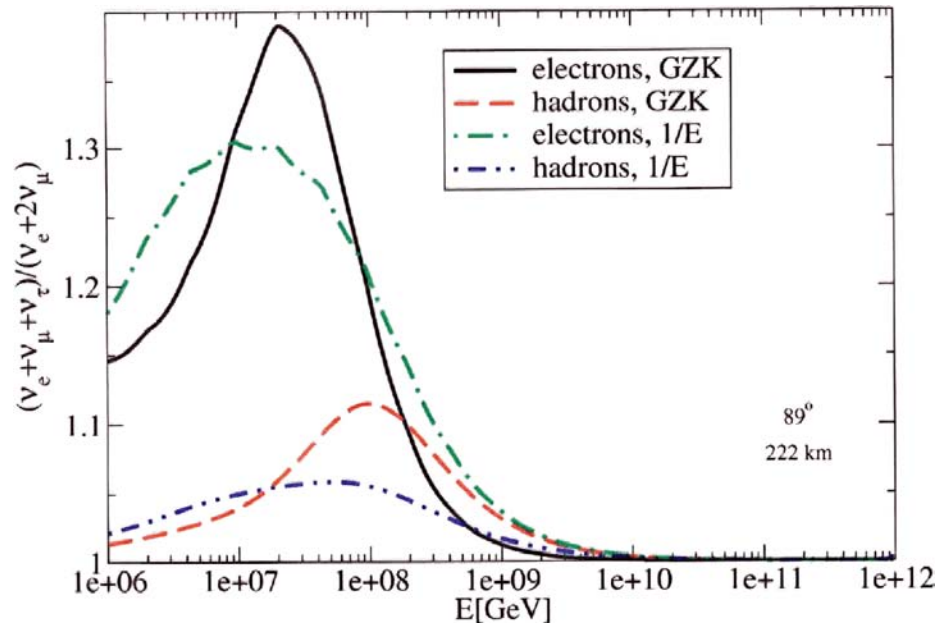


Figure 19: Ratio of electromagnetic and hadronic shower rates in the presence and absence of $\nu_\mu \rightarrow \nu_\tau$ oscillations for GZK and $1/E$ fluxes of neutrinos for detection over 222 km of ice.

19

Detection of Cosmic Neutrinos

- Muon tracks (IceCube, RICE)
- Electromagnetic and Hadronic Showers (IceCube, RICE, ANITA, Auger, OWL, EUSO)
- To determine the energy flux (muons or showers) that reaches the detector we need to consider propagation of neutrinos and leptons through the Earth and ice
- ν_τ give different contribution from ν_μ due to the very short τ lifetime, i.e. the regeneration effect.

Observables: showers in ice

- Electromagnetic showers:

Tau decay: $\tau \rightarrow e + \bar{\nu}_e + \nu_\tau$

ν_e CC interactions: $\nu_e + N \rightarrow e + X$

- Hadronic showers

Tau decay: $\tau \rightarrow \nu_\tau + X$

ν_τ NC interactions: $\nu_\tau + N \rightarrow \nu_\tau + X$

ν_τ CC interactions: $\nu_\tau + N \rightarrow \tau + X$

$\nu_{e,\mu}$ NC and CC interactions

Electromagnetic Showers from Tau Decays

- Decay of taus produced outside the detector that decay electromagnetically inside the detector ("lollipop" events in IceCube and em showers in RICE)

$$F_{sh,\tau}^{em,1}(E_e) = B_{\tau \rightarrow e} \int_{E_e} dE_\tau \int dx F_\tau(E_\tau) e^{-x/\lambda_\tau^{dec}} \frac{1}{\lambda_\tau^{dec}} \frac{dn_{\tau \rightarrow e}}{dE_e}(E_\tau e^{-\beta x}, E_e)$$

- Taus produced and decay electromagnetically inside the detector ("double bang" events in IceCube)

$$\begin{aligned} F_{sh,\tau}^{em,2}(E_e) = & B_{\tau \rightarrow e} \int_0^{dp} dx \int_x^{dp} dy \int_{E_e}^{E_{max}} dE_{\nu_\tau} \int_{E_e}^{E_\nu} dE_\tau F_{\nu_\tau}(E_{\nu_\tau}) \times \\ & \times e^{-x N_A \sigma^{CC}(E_\nu)} N_A \frac{d\sigma^{CC}}{dE_\tau}(E_{\nu_\tau}, E_\tau) \times \\ & \times e^{-y/\lambda_\tau^{dec}(E_\tau e^{-\beta y})} \frac{1}{\lambda_\tau^{dec}(E_\tau e^{-\beta y})} \frac{dn_{\tau \rightarrow e}}{dE_e}(E_e, E_\tau e^{-\beta y}) \end{aligned}$$

- Electromagnetic showers from the ν_e CC interactions

$$F_{sh,\nu}^{em} = \int_{E_e}^{E_{max}} dE_\nu F_\nu(E_\nu) (1 - e^{-d\rho N_A \sigma^{CC}(E_\nu)}) \left[\frac{1}{\sigma^{CC}(E_\nu)} \frac{d\sigma^{CC}}{dE_e}(E_\nu, E_e) \right]$$

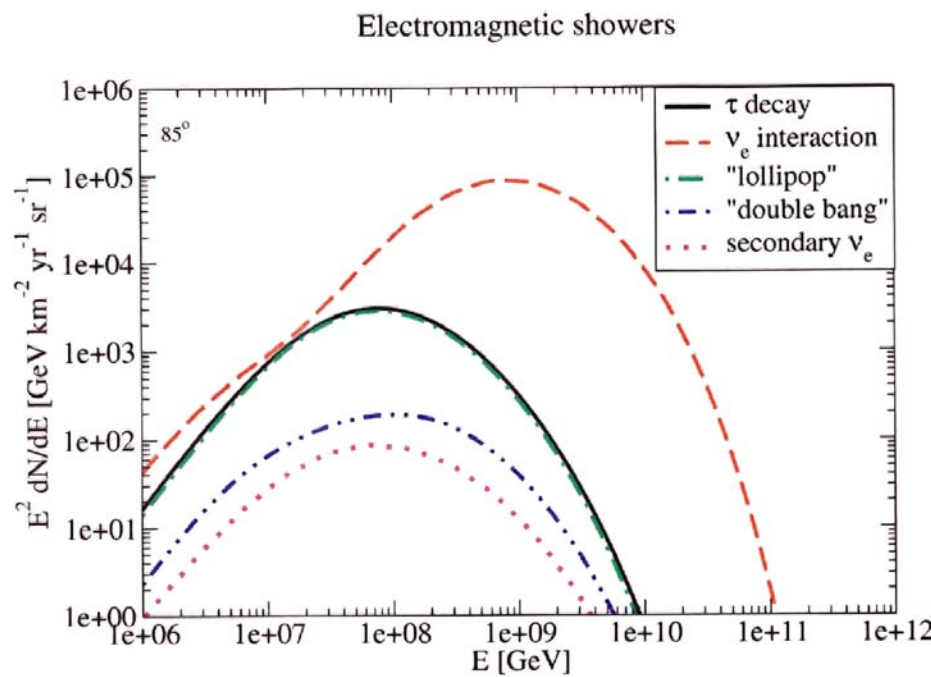


Figure 8: Electromagnetic shower distributions for GZK neutrinos, at a nadir angle of 85° for a km size detector. The τ decay curve is the sum of the lollipop and double bang curves.

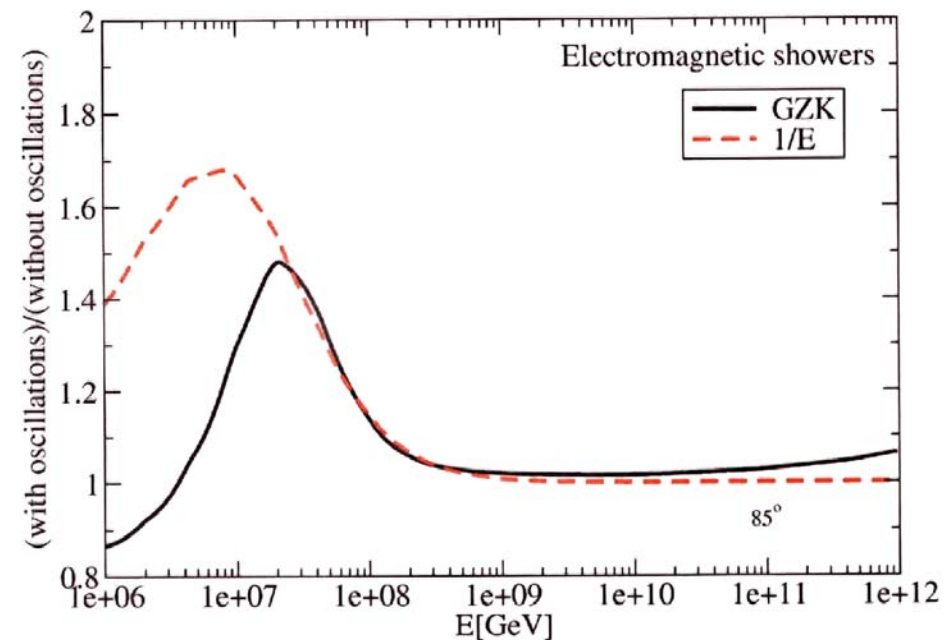


Figure 10: Ratio of electromagnetic shower rates in the presence and absence of $\nu_\mu \rightarrow \nu_\tau$ oscillations for GZK and $1/E$ neutrino spectra for nadir angle 85° for a km size detector.

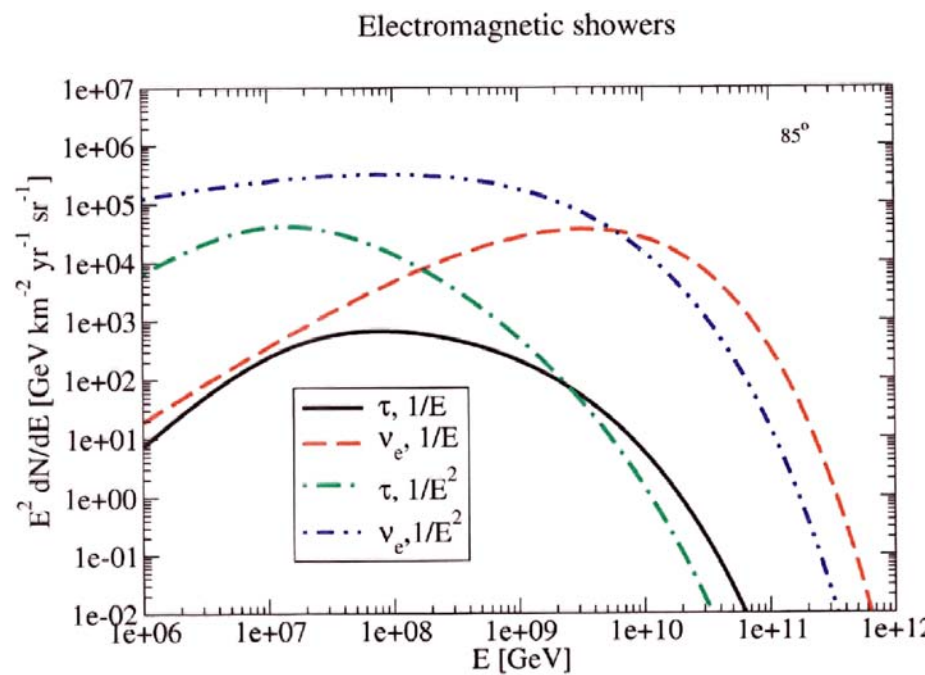


Figure 13: Electromagnetic shower distributions for nadir angle 85° for $1/E$ and $1/E^2$ characteristic fluxes for a km size detector from ν_e interactions and from τ decays.

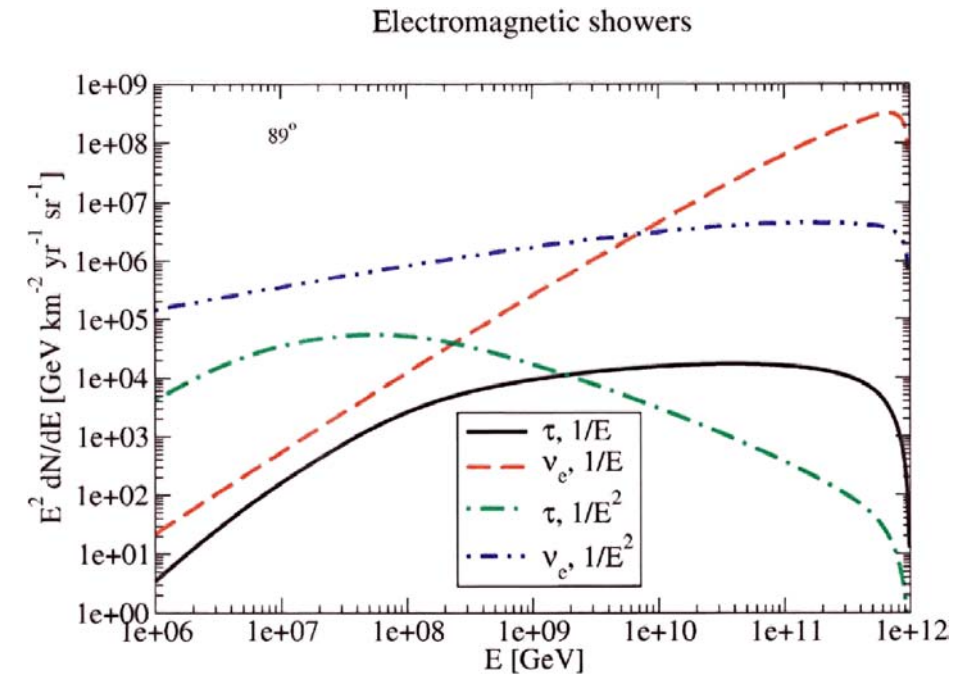


Figure 14: Electromagnetic shower distributions for nadir angle 89° for $1/E$ and $1/E^2$ characteristic fluxes for a km size detector.

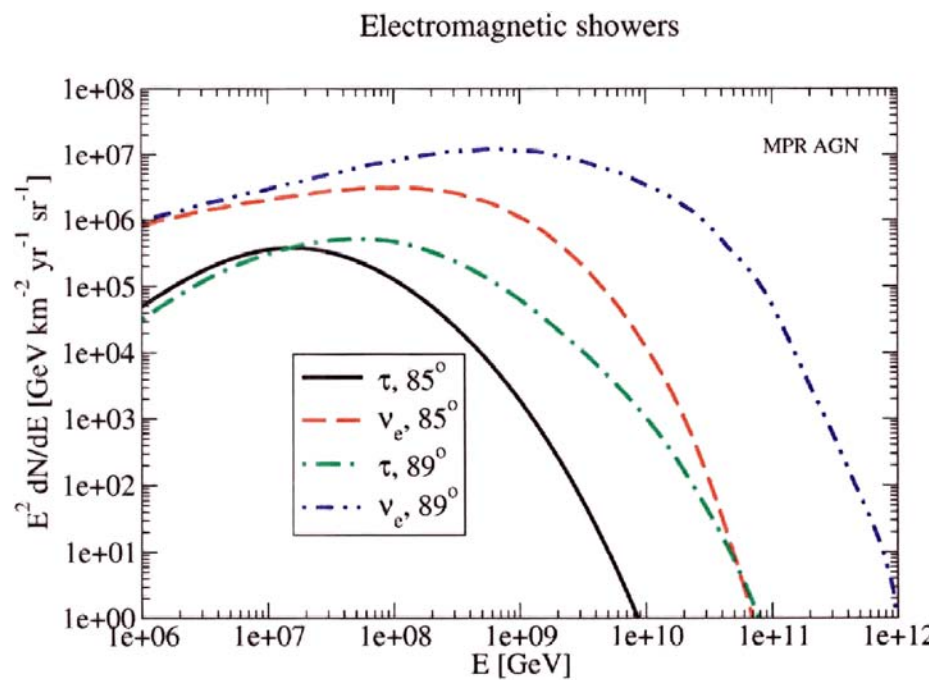


Figure 16: Electromagnetic shower distributions for the MPR AGN model for a km size detector.

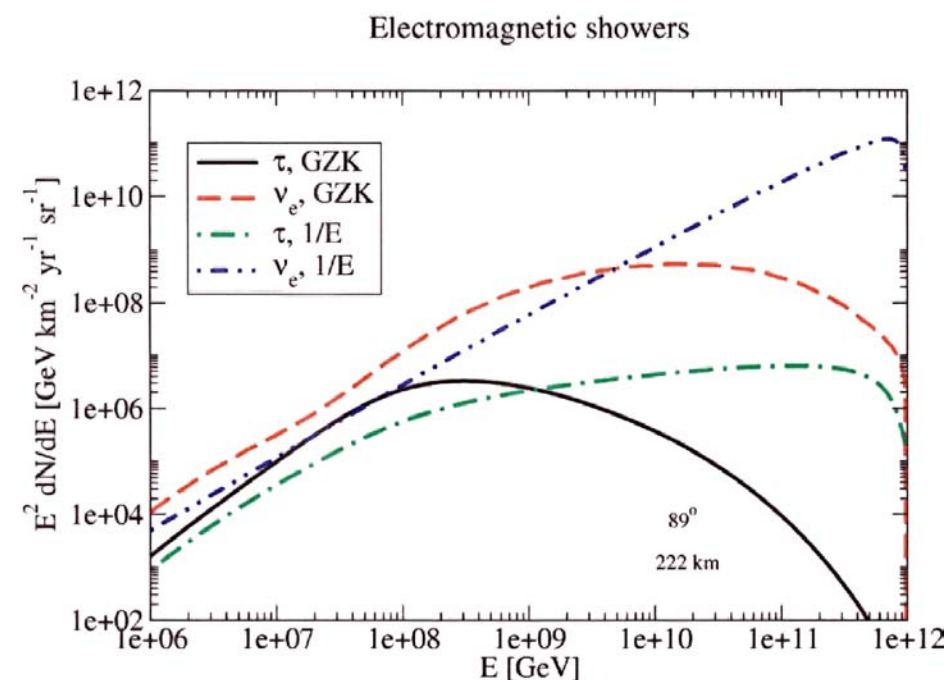


Figure 17: Electromagnetic shower distributions for detection over 222 km of ice.

Hadronic Showers from Tau Decays

- Decay of taus produced outside the detector that decay hadronically inside the detector ("lollipop" events in IceCube and em showers in RICE)

$$F_{sh,\tau}^{h,1}(E_h) = B_{\tau \rightarrow h} \int_{E_h} dE_\tau \int dx F_\tau(E_\tau) e^{-x/\lambda_\tau^{dec}} \frac{1}{\lambda_\tau^{dec}} \frac{dn_{\tau \rightarrow h}}{dE_h}(E_\tau e^{-\beta x}, E_h)$$

- Taus produced and decay hadronically inside the detector ("double bang" events in IceCube)

$$\begin{aligned} F_{sh,\tau}^{h,2}(E_h) = & B_{\tau \rightarrow h} \int_0^{d\rho} dx \int_x^{d\rho} dy \int_{E_h}^{E_{max}} dE_{\nu_\tau} \int_{E_h}^{E_\nu} dE_\tau F_{\nu_\tau}(E_{\nu_\tau}) \times \\ & \times e^{-x N_A \sigma^{CC}(E_\nu)} N_A \frac{d\sigma^{CC}}{dE_\tau}(E_{\nu_\tau}, E_\tau) \times \\ & \times e^{-y/\lambda_\tau^{dec}(E_\tau e^{-\beta y})} \frac{1}{\lambda_\tau^{dec}(E_\tau e^{-\beta y})} \frac{dn_{\tau \rightarrow h}}{dE_h}(E_h, E_\tau e^{-\beta y}) \end{aligned}$$

- Hadronic showers from the ν_e , ν_μ and ν_τ CC interactions

$$F_{sh,\nu}^h = \int_{E_h}^{E_{max}} dE_\nu F_\nu(E_\nu) (1 - e^{-d\rho N_A \sigma^{CC}(E_\nu)}) \left[\frac{1}{\sigma^{CC}(E_\nu)} \frac{d\sigma^{CC}}{dE_h}(E_\nu, E_h) \right]$$

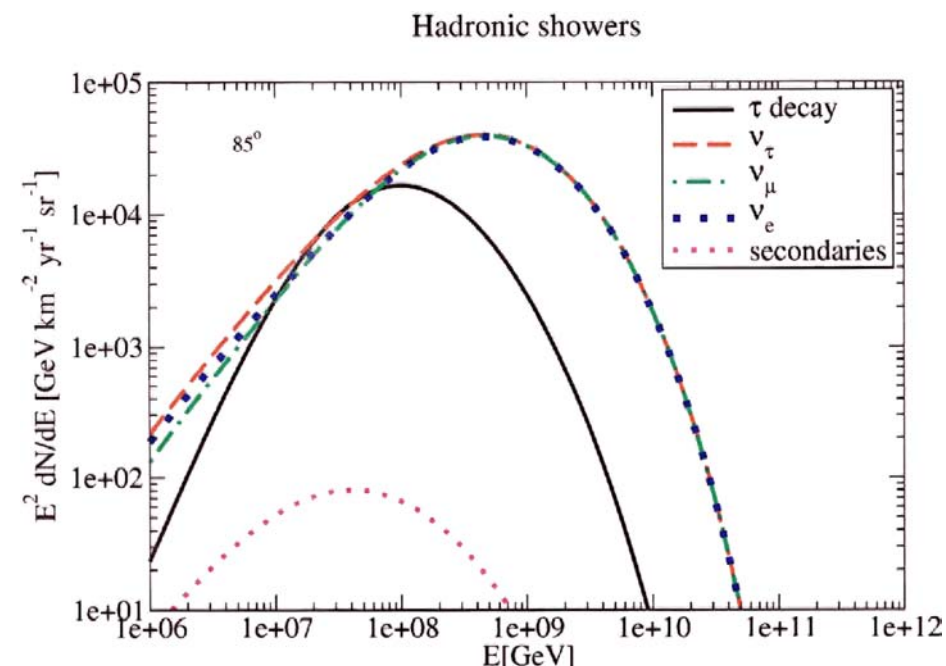
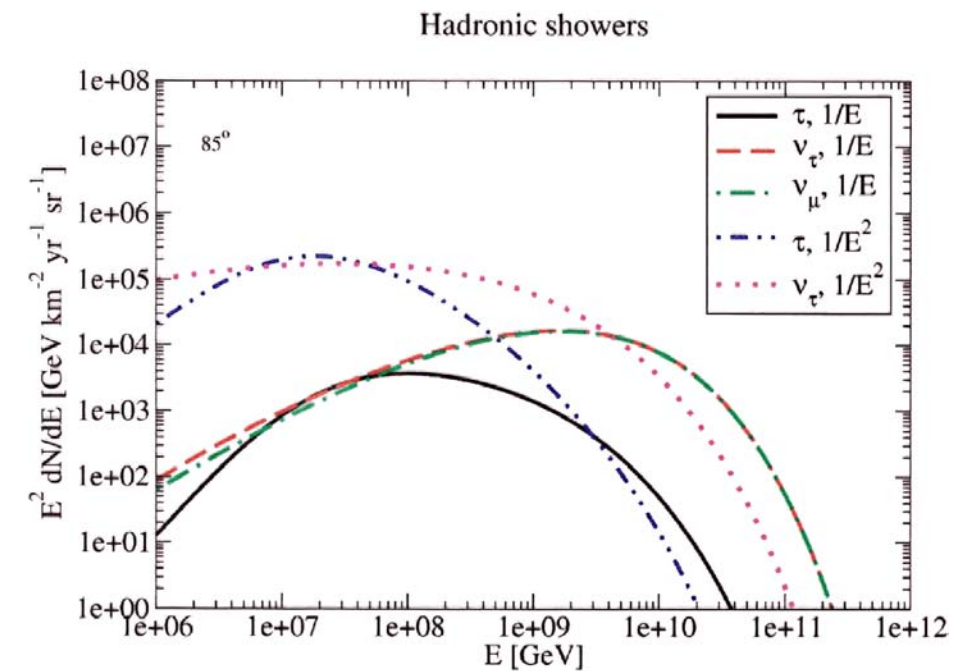
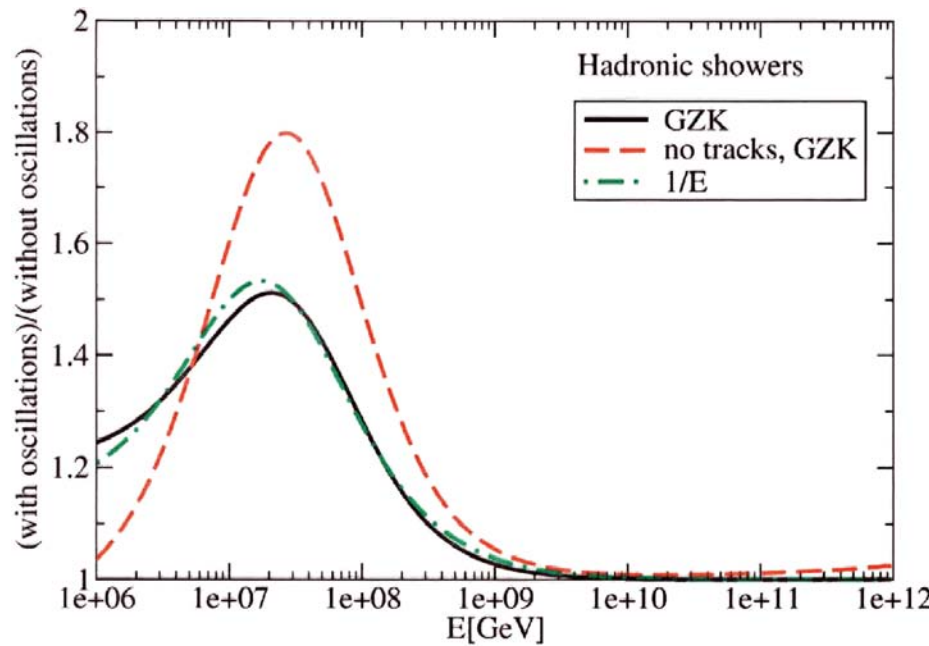


Figure 9: Hadronic shower distributions for GZK neutrinos, at a nadir angle of 85° for a km size detector.



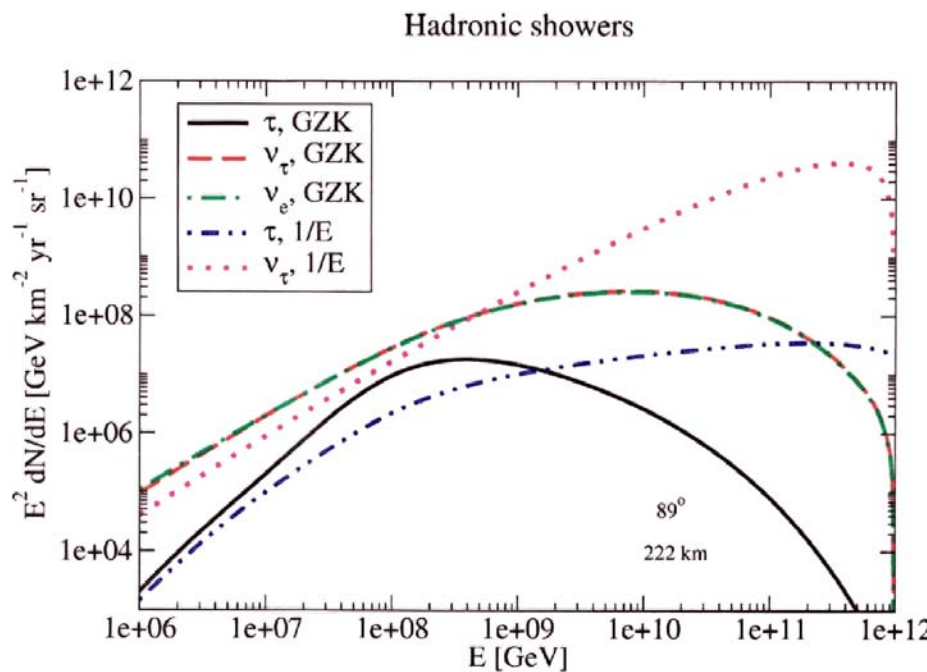


Figure 18: Hadronic shower distributions for detection over 222 km of ice. The ν_μ distribution for GZK neutrinos is the same with that of ν_τ . For the $1/E$ flux all neutrino distributions are almost the same.

18

- Very high energy cosmic neutrinos also present unique opportunity to study the interactions of elementary particles at energies beyond those obtainable in current or planned colliders.

- Cosmic neutrinos with energies E_ν above 10^{17} eV probe neutrino-nucleon scattering at center-of-mass (c.m.) energies above

$$\sqrt{s_{\nu N}} \equiv \sqrt{2m_N E_\nu} \simeq 14 \left(\frac{E_\nu}{10^{17} \text{ eV}} \right)^{1/2} \text{ TeV}$$

- These energies are beyond the proton-proton c.m. energy $\sqrt{s_{pp}} = 14$ TeV of the LHC, and Bjorken- x values below

$$x \simeq 2 \times 10^{-4} \left(\frac{Q^2}{m_W^2} \right) \left(\frac{0.2}{y} \right) \left(\frac{10^{17} \text{ eV}}{E_\nu} \right)$$

Neutrinos as Probes of New Particle Physics

- Enhancements in the νN cross section due to physics beyond the Standard Model, such as
 - * Electroweak instanton-induced processes,
 - * Microscopic black holes as predicted in TeV scale gravity models
 - * Exchange of Kaluza-Klein gravitons
- Probing low scale Supersymmetry with neutrinos: production of charged sleptons in HE neutrino interactions
- Measurements of neutrino interactions at extremely high energies \Rightarrow powerful tests of fundamental physics at and beyond a scale of 1-10TeV.

- Detection of HE neutrinos with neutrino telescopes depends strongly on neutrino interactions and their cross section:

- Event rates for *downward* muons (leptons/sleptons or hadrons) from neutrino interactions:

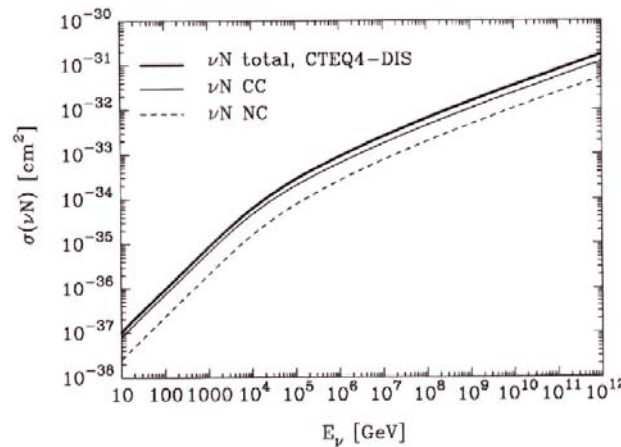
$$R_\nu = V \int dE_\nu \sigma_{cc}(E_\nu) F_\nu(E_\nu)$$

- Event rates for *upward* muons (leptons/sleptons) from neutrino interactions:

$$R_\nu = A N_A / dE_\nu R(E_\nu, E_\mu) \sigma_{cc}(E_\nu) S(E_\nu) F_\nu(E_\nu, X)$$

where $R(E_\nu, E_\mu)$ is the muon range and $S(E_\nu)$ is the neutrino attenuation factor.

- Standard Model neutrino interaction cross section is small. At low energies SM neutrino cross section is under control thanks to HERA measurements of the structure functions. At higher energies, we require knowledge of small x parton distributions \Rightarrow DGLAP/BFKL approach including non-linear effects.



R. Gandhi, C. Quigg, M.H. Reno and I.S., PRD58, 093009 (1998)

- In addition, “new physics” (i.e. physics beyond the SM) can alter neutrino interactions.

Signals of Electroweak Instantons in Neutrino Telescopes

- Instantons are non-perturbative gauge field fluctuations that describe tunnelling transitions between different topological configurations in non-abelian gauge theories like electroweak theory or like QCD.
- Instanton induced neutrino-nucleon cross section becomes dominant over the standard model charged-current cross section at energies above 10^9 GeV.

Probing Extra Dimensions with Neutrinos

- Possibility that we live in $4 + n$ spacetime dimensions has profound implications. If gravity propagates in these extra dimensions, the fundamental Planck scale, M_D , at which gravity becomes comparable in strength to other forces, may be in TeV range, leading to a host of potential signatures for high energy physics \Rightarrow one of the most striking consequences of low-scale gravity is the possibility of black hole creation in high-energy particle collisions.
- Gravitation processes involving graviton emission and exchange, analyses rely on a perturbative description that breaks down for energies of M_D and above.
- In contrast, black hole properties are best understood for energies above M_D , where semiclassical and thermodynamic descriptions become increasingly valid.

- Copious production of microscopic black holes is one of the least model-dependent predictions of TeV-scale gravity scenarios.
- Ultrahigh energy neutrinos ($E_\nu > 100$ TeV) can provide unique probe of the large extra spacetime dimensions \Rightarrow detection of the black hole formation in neutrino interactions would reveal the structure of the extra dimensions on scales large as compared to the Planck scale.
- Large-scale neutrino telescopes, such as ICECUBE, ANTARES and NESTOR, ground shower arrays and fluorescence detectors, such as Fly's Eye, AGASA and Auger and the satellite experiments, such as EUSO and OWL have potentials to detect black holes. These detectors are most sensitive to showers and muons from the evaporation of black holes.

Black Hole Production by UHE Neutrinos

- Black hole can be produced in scattering of UHE neutrinos on nucleons in the atmosphere or in the Earth. The neutrino-nucleon cross section for black hole production is given by

$$\sigma(\nu N \rightarrow \text{BH}) = \sum_i \int_{M_{BH}^{\min}}^1 dx \hat{\sigma}_i(xs) f_i(x, Q^2),$$

where

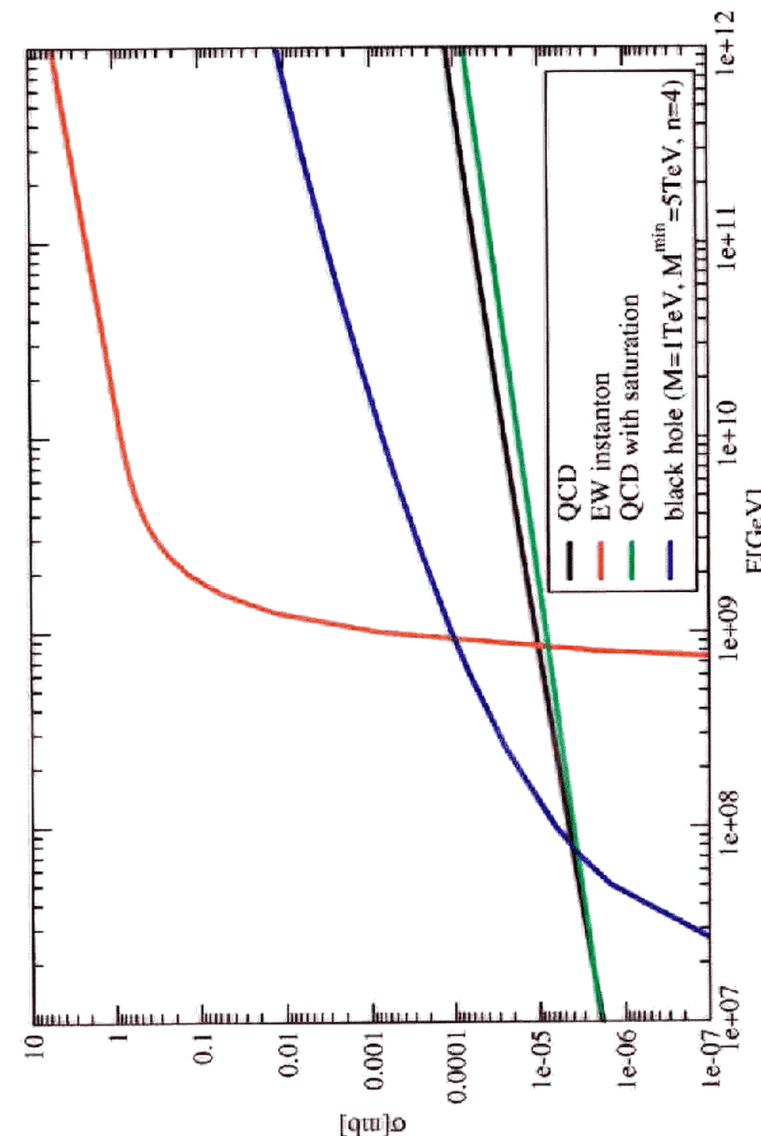
$$\hat{\sigma}_i = \pi r_S^2(M_{BH} = \sqrt{\hat{s}}) \theta(\sqrt{\hat{s}} - M_{BH}^{\min}),$$

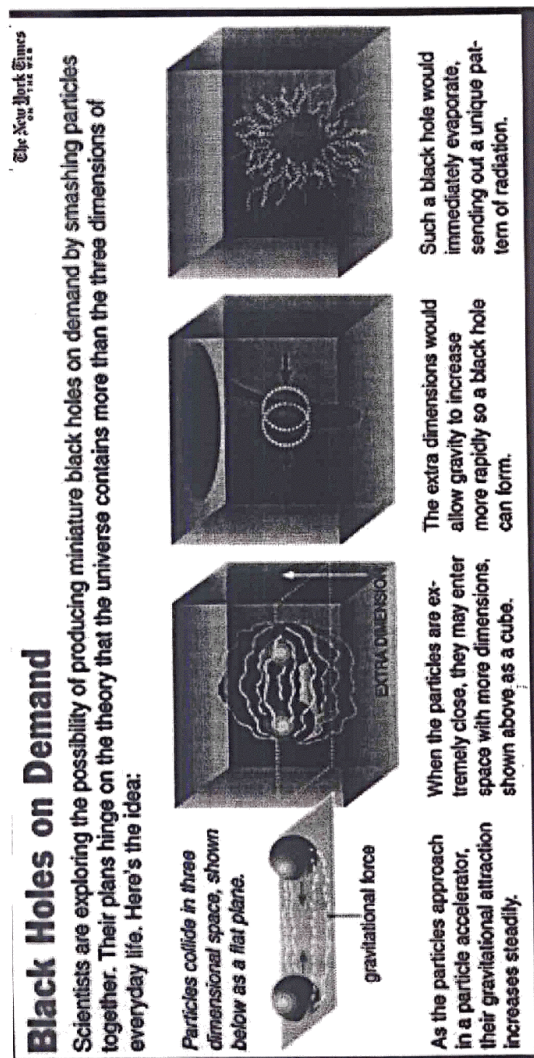
$\hat{s} = xs$, s is the center of mass energy, $s = 2m_N E_\nu$

$f_i(x, Q^2)$'s are parton distribution functions

M_{BH}^{\min} is the minimum black hole mass for which

semiclassical approximation above is valid ($M_{BH}^{\min} \gg M_D$)





UHE Neutrinos as Probes of New Physics

- Even before the LHC, new TeV-scale physics may be observed in the scattering of ultrahigh energy ($E_\nu > 100 \text{ TeV}$) cosmic or extragalactic neutrinos off nuclei in air or ice and detected by neutrino telescopes such as **AMANDA**, **ICECUBE** or **RICE** or by balloon experiment, such as **ANITA** or with cosmic ray air shower detectors such as **Pierre Auger** or **AGASA** or with the satellite experiments, such as **EUSO** and **OWL**.

Black Holes in Cosmic Rays

Feng and Shapere, PRL 88 (2002) 021303.
 Anchordoqui, Feng, Goldberg and Shapere,
 PR D65 (2002) 124027.

- Limits from non-observation of horizontal showers by the Fly's Eye Collaboration and Akeno Giant Air Shower Array (AGASSA): $M_D \approx 1\text{TeV} - 1.4\text{ TeV}$ excluded for $n \geq 4$.
- Detect BH in the Pierre Auger fluorescence experiment or AGASSA \Rightarrow few to a hundred BHs can be detected before the LHC turns on. If no black holes are found then $M_D = 2\text{ TeV}$ is excluded for any n .

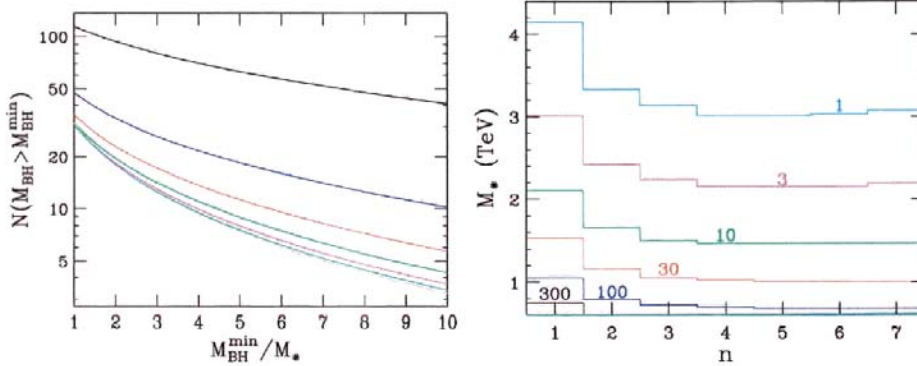


Figure 1: The number of BH events detected in 5 Auger site-years a) $M_* = 1\text{TeV}$; b) $M_* = M_{BH}^{\min}$

Black Holes in Neutrino Telescopes

Alvarez-Muniz, Feng, Halzen, Tan and Hooper,
 PRD 65, 124015 (2002)
 Kowalski, Ringwald and Tu, PL B529, 1 (2002)
 Dutta, Reno and Sarcevic, PR D66, 033002 (2002)

- The contained event rate for black hole production is

$$\text{Rate} = \int dE_\nu N_A V_{eff} \sigma_{BH}(E_\nu) \frac{dN_\nu}{dE_\nu}$$

N_A is Avogadro's number

$\frac{dN_\nu^\mu}{dE_\nu^\mu}$ is the neutrino flux that reaches the detector

V_{eff} is the effective volume of the detector.

Event Rates for ICECUBE

Contained event rates per year for $M_D = 1$ TeV ($m = M_{BH}^{\min}/M_D$) and $E_{\text{sho}}^{\min} = 10^8$ GeV.

$n = 4$

m	E^{-1}	E^{-2}	GRB_{WB}	TD_{WMB}	TD_{SLSC}	AGN_{M95}	AGN_{SS}	COS_{STD}	COS_{STR}
1	5447.0	444.3	0.481	56.01	0.563	32.73	9.348	2.16	5.89
2	2430.0	225.0	0.206	34.30	0.285	15.96	3.767	1.19	3.16
3	1363.0	141.1	0.112	24.77	0.177	9.65	1.923	0.79	2.06
4	848.2	97.9	0.067	19.26	0.121	6.45	1.082	0.57	1.47
5	560.0	72.0	0.043	15.65	0.088	4.57	0.636	0.43	1.11

$n = 6$

m	E^{-1}	E^{-2}	GRB_{WB}	TD_{WMB}	TD_{SLSC}	AGN_{M95}	AGN_{SS}	COS_{STD}	COS_{STR}
1	9930.0	797.9	0.879	97.46	1.013	59.14	17.190	3.85	10.50
2	4161.0	378.8	0.355	55.99	0.481	27.07	6.514	1.98	5.29
3	2250.0	228.5	0.186	38.92	0.288	15.76	3.210	1.26	3.32
4	1364.0	154.0	0.109	29.45	0.192	10.25	1.762	0.89	2.31
5	881.7	110.9	0.068	23.42	0.137	7.12	1.016	0.66	1.71
SM	136	8.4	0.01	0.65	0.01	0.6	0.3	0.03	0.09

Contained event rates per year for $M_D = 2$ TeV and $E_{\text{sho}}^{\min} = 10^8$ GeV.

$n = 4$

m	E^{-1}	E^{-2}	GRB_{WB}	TD_{WMB}	TD_{SLSC}	AGN_{M95}	AGN_{SS}	COS_{STD}	COS_{STR}
2	460.3	42.63	0.39E-01	6.50	0.54E-01	3.023	0.71E+00	0.225	0.599
4	160.7	18.54	0.13E-01	3.65	0.23E-01	1.222	0.21E+00	0.108	0.279
6	72.7	10.47	0.54E-02	2.48	0.13E-01	0.639	0.72E-01	0.065	0.165
8	36.2	6.68	0.24E-02	1.85	0.77E-02	0.375	0.23E-01	0.044	0.109
10	19.9	4.65	0.12E-02	1.45	0.51E-02	0.238	0.91E-02	0.031	0.077

$n = 6$

m	E^{-1}	E^{-2}	GRB_{WB}	TD_{WMB}	TD_{SLSC}	AGN_{M95}	AGN_{SS}	COS_{STD}	COS_{STR}
2	853.3	77.67	0.73E-01	11.48	0.99E-01	5.551	0.13E+01	0.406	1.085
4	279.7	31.59	0.22E-01	6.04	0.39E-01	2.103	0.36E+00	0.182	0.474
6	121.9	17.11	0.90E-02	3.95	0.21E-01	1.058	0.12E+00	0.106	0.269
8	58.9	10.59	0.39E-02	2.86	0.12E-01	0.604	0.39E-01	0.069	0.173
10	31.8	7.19	0.20E-02	2.19	0.80E-02	0.375	0.15E-01	0.048	0.119
SM	136	8.4	0.01	0.65	0.01	0.6	0.3	0.03	0.09

Contained event rates per year for $M_D = 3\text{TeV}$ and $E_{sh}^{\min} = 10^8 \text{ GeV}$.

$n = 4$

m	E^{-1}	E^{-2}	GRB_{WB}	TD_{WMB}	TD_{SLSC}	AGN_{M95}	AGN_{SS}	COS_{STD}	COS_{STR}
3	97.6	10.11	0.80E-02	1.77	0.13E-01	0.691	0.14E+00	0.56E-01	0.15E+00
6	27.5	3.96	0.20E-02	0.94	0.48E-02	0.241	0.27E-01	0.25E-01	0.62E-01
9	9.9	2.08	0.61E-03	0.62	0.24E-02	0.112	0.47E-02	0.14E-01	0.34E-01
12	4.4	1.30	0.23E-03	0.45	0.13E-02	0.061	0.66E-03	0.88E-02	0.22E-01
15	2.0	0.88	0.98E-04	0.34	0.81E-03	0.035	0.11E-03	0.60E-02	0.14E-01

$n = 6$

3	182.6	18.55	0.15E-01	3.16	0.23E-01	1.280	0.26E+00	0.10E+00	0.27E+00
6	48.2	6.77	0.36E-02	1.56	0.82E-02	0.419	0.49E-01	0.42E-01	0.11E+00
9	16.6	3.42	0.10E-02	0.98	0.39E-02	0.187	0.80E-02	0.23E-01	0.56E-01
12	7.1	2.06	0.38E-03	0.70	0.22E-02	0.099	0.11E-02	0.14E-01	0.34E-01
15	3.2	1.36	0.16E-03	0.52	0.13E-02	0.056	0.17E-03	0.94E-02	0.22E-01

SM	136	8.4	0.01	0.65	0.01	0.6	0.3	0.03	0.09
----	-----	-----	------	------	------	-----	-----	------	------

Detection of Black Holes with OWL

Dutta, Reno and Sarcevic, PR D66, 033002 (2002)

The event rate for black hole production with OWL is given by

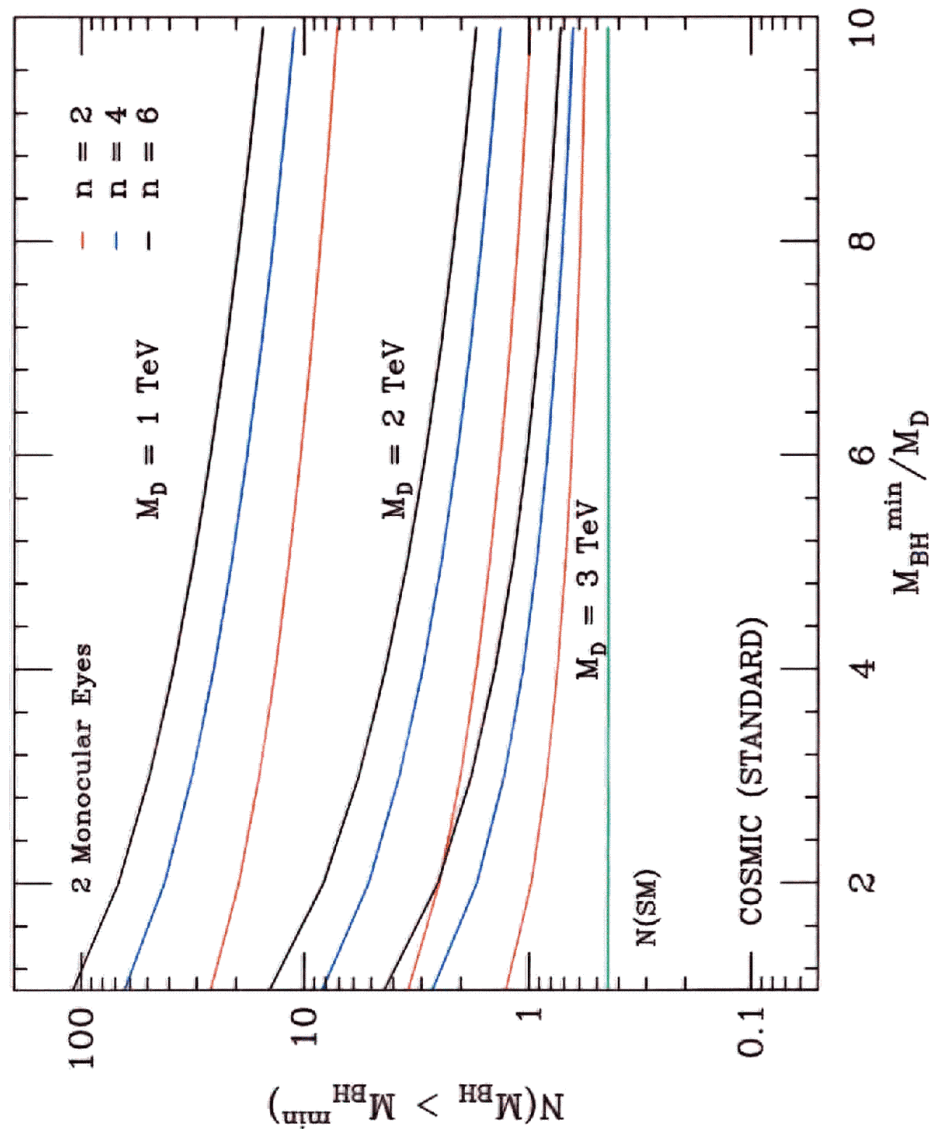
$$N = \int A(E_\nu) \frac{dN}{dE_\nu} \sigma_{BH}(E_\nu) dE_\nu$$

where

$A(E_\nu)$ is the OWL effective aperture

$\frac{dN}{dE_\nu}$ is the neutrino flux

$\sigma_{BH}(E_\nu)$ is the cross section for the production of black hole.



- UHE neutrino interactions can probe physics scales above TeV \Rightarrow potential for discovering physics beyond the Standard Model.
- Production of black holes in νN interactions exceeds Standard Model cross section at energies above 10^8 GeV for $M_D \geq 2 \text{ TeV}$ and $n \geq 2$.
- Black Holes in Cosmic Rays: Limits from Fly's Eye and AGASSA, $M_D \approx 1 \text{ TeV} - 1.4 \text{ TeV}$ excluded for $n \geq 4$. Pierre Auger experiment can probe $M_D \leq 2 \text{ TeV}$ for any n .
- Black Holes with Neutrino Telescopes: ICECUBE rates for BH detection are promising for AGN and TD Models (for $M_D \leq 2 \text{ TeV}$, $n \geq 2$) but rates for cosmogenic neutrinos are too small.
- OWL could potentially probe the fundamental Planck scale up to $M_D = 3 \text{ TeV}$ for $n \geq 2$.

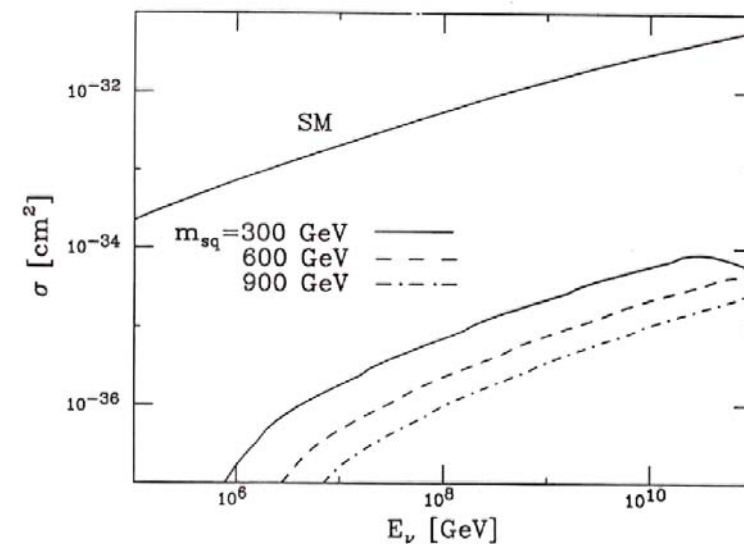
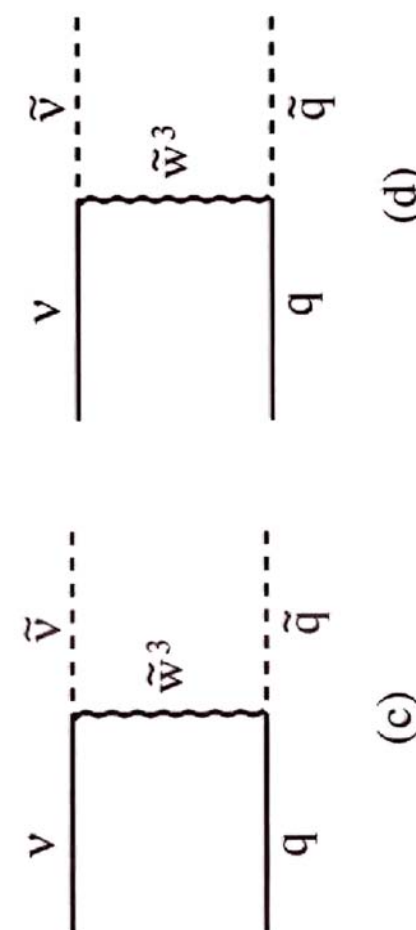
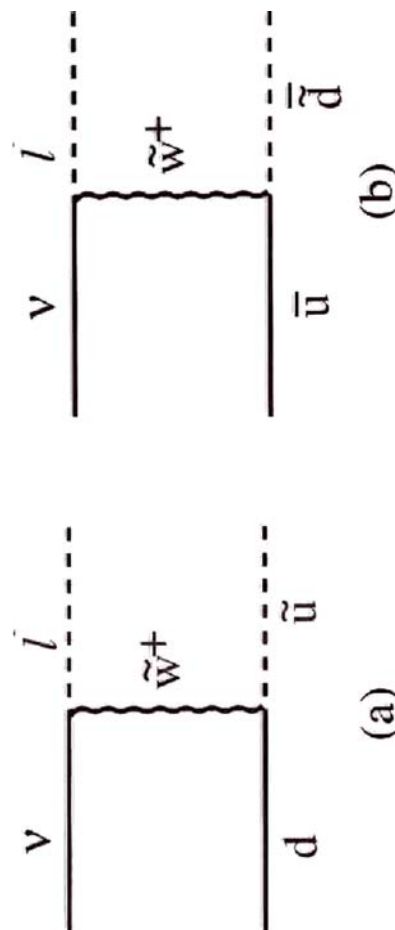
Probing Supersymmetry with Neutrinos

I. Albuquerque, G. Burdman, Z. Chacko, PRL 92 (2004)

M.H. Reno, I.S. and S. Su, hep-ph/0503030

- In low scale supersymmetric models, lightest supersymmetric particle (LSP) is the gravitino. NSLP is typically a long lived charged slepton.
- Collisions of high energy neutrinos with nucleons in the earth can result in the production of sleptons. Their very high boost means they travel very long distances before decaying.
- Sleptons traverse the earth losing their energy via bremsstrahlung, pair production and photonuclear interactions. Energy dependence of the energy loss translates into energy spectrum of the staus that reach the detector where they decay.

- The energy spectrum of stau at the detector depends on initial neutrino flux, neutrino-nucleon interactions and on slepton energy loss.
- Neutrino telescopes (ICECUBE, ANITA) have unique ability to provide the first evidence for supersymmetry at weak scale.



νN cross sections vs. the energy of the incident neutrino. The curves correspond to $m_{\tilde{\ell}_L} = 250$ GeV, $m_{\tilde{w}} = 250$ GeV; and for squark masses $m_{\tilde{q}} = 300$ GeV (solid), 600 GeV (dashed) and 900 GeV (dot-dashed). The top curve corresponds to the SM charged current interactions

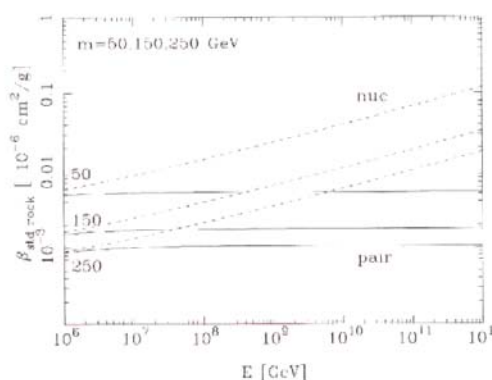
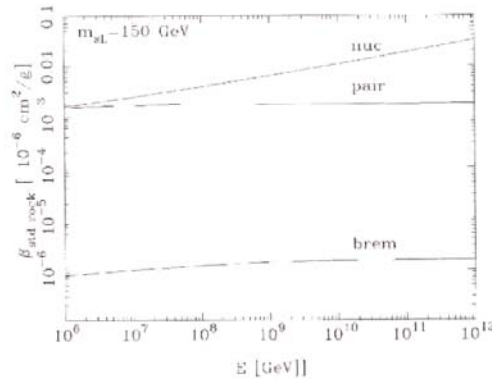
I. Albuquerque, G. Burdman and Z. Chacko,
Phys. Rev. Lett. 92, 221802 (2004).

Energy Loss of Stau

The average energy loss of a stau traversing a distance X

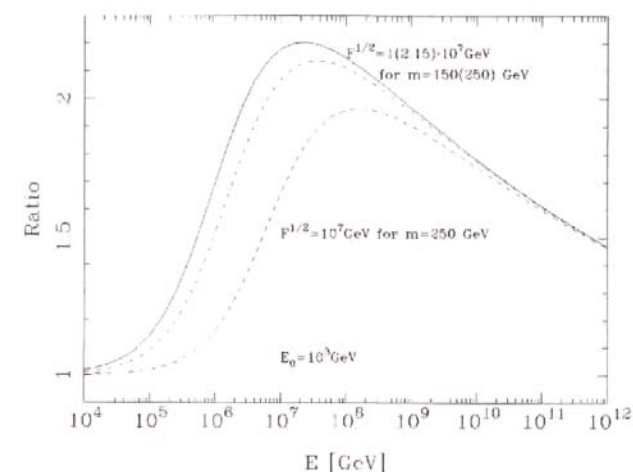
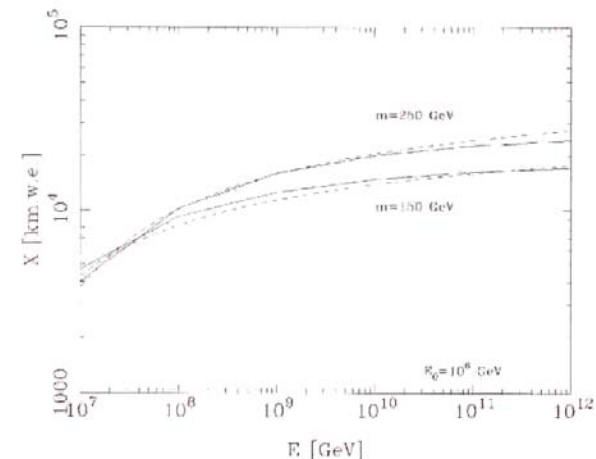
$$-\langle \frac{dE}{dX} \rangle = \alpha + \beta E$$

where α is the ionization energy loss, and β is the radiative energy loss.

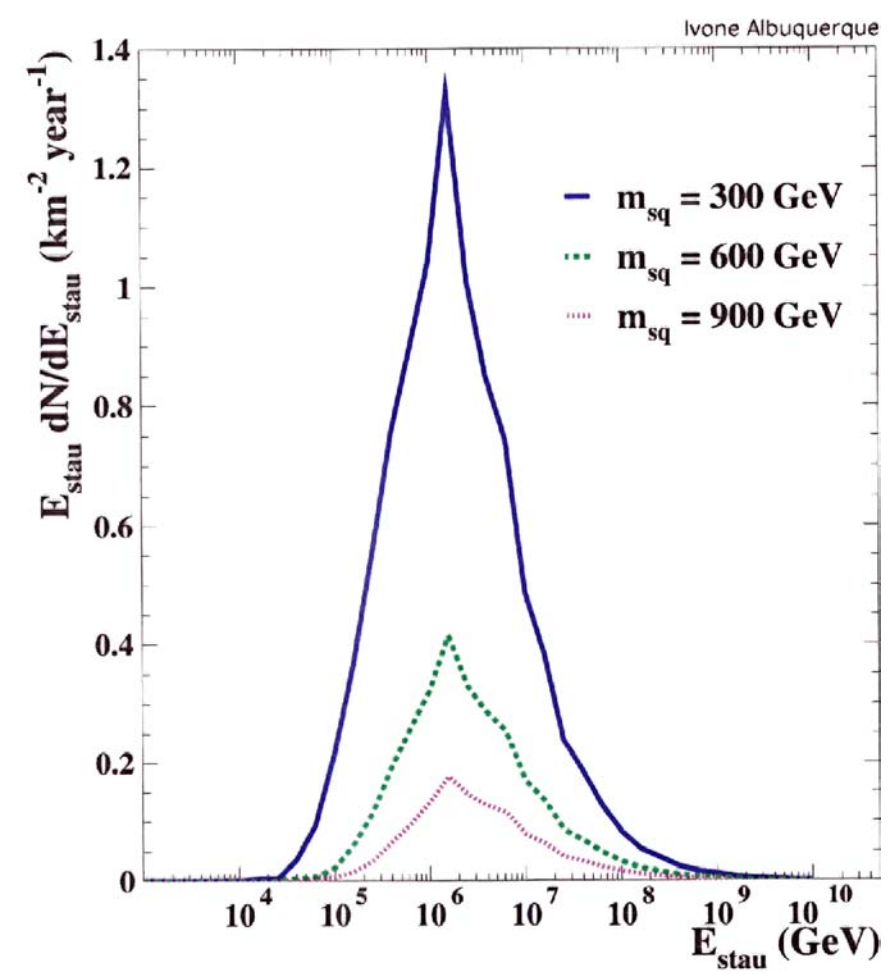
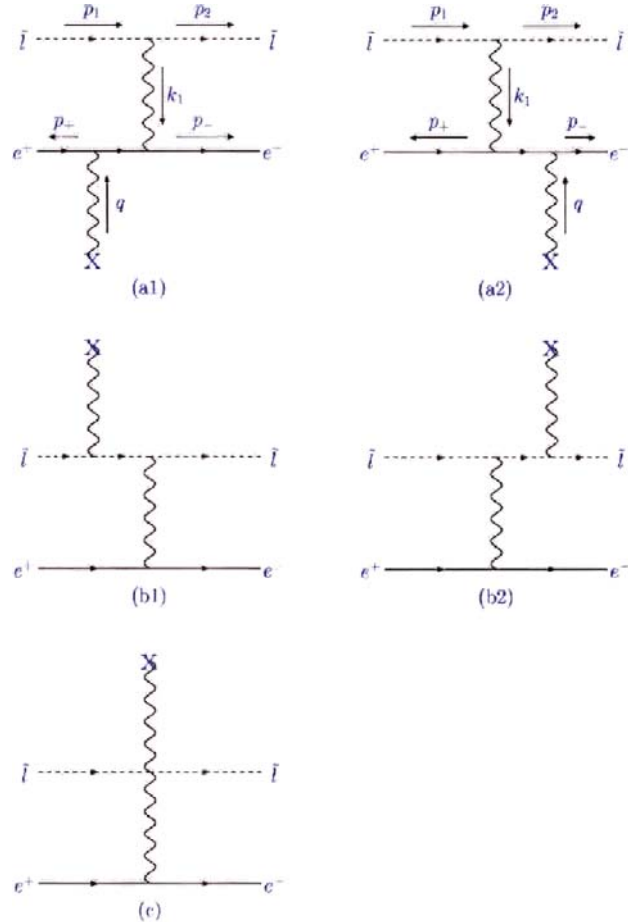


M.H. Reno, I.S. and S. Su, hep-ph/050303C

Stau Range



M.H. Reno, I.S. and S. Su, hep-ph/050303C



M.H. Reno, I.S. and S. Su, hep-ph/0503030

Summary

- Above 10^8 GeV, tau energy loss is important.
- For $E_\nu > 10^8$ GeV, ν_τ flux resembles ν_μ flux, due to the tau energy loss.
- Below 10^8 GeV, regeneration of ν_τ becomes important while ν_μ are strongly attenuated.
- The regeneration effect depends strongly on the shape of the initial flux and it is larger for flatter fluxes.
- The enhancement due to regeneration also depends on the amount of material traversed by neutrinos and leptons, i.e. on nadir angle.

- Neutrinos provide a new window to the Universe
 - High energy neutrinos are unique probes of particle physics, astrophysics and cosmology
 - High energy neutrinos probe new energy and density regimes
 - High energy neutrino telescopes may reveal existence of interactions induced by standard model electroweak instantons, or **physics beyond the standard model** (low scale supersymmetry, TeV scale gravity, extra dimensions...)
- IceCube, Rice, ANITA, OWL, Euso, Auger, SALSA, LOFAR ...